

ОБЪЕДИНЕННЫЙ
ИНСТИТУТ
ЯДЕРНЫХ
ИССЛЕДОВАНИЙ
ДУБНА

M-37
E17-88-66

D.Mihalache¹, R.G.Nazmitdinov², V.K.Fedyanin

**NONLINEAR OPTICAL WAVES
IN LAYERED STRUCTURES**

Submitted to "ЭЧАЯ"

¹ Central Institute of Physics, Department of
Fundamental Physics, P.O.Box MG-6, Bucharest,
Romania.

² Institute of Applied Physics, Tashkent State
University, Tashkent, USSR.

1988

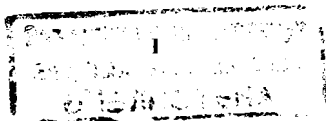
1. Introduction

The discovery of optical bistability in semiconductors such as GaAs ^{/1/} and InSb ^{/2/} with its multiplicity of applications to all-optical signal processing systems for optical communications and optical computing stimulated a great deal of theoretical and experimental activity in the late few years (see ^{/3-4/}). Nonlinear optical devices such as bistable switches ^{/1-2/}, logic gates ^{/5-6/}, etc., have been already demonstrated in a plane wave context. Planar optical waveguide with their inherent confinement of the light in one dimension of the order of wavelength of light provides the optimum geometry of performing efficient nonlinear interaction in general and nonlinear optical signal processing in particular.

The key concept in which all nonlinear guided wave optical devices are based is that the local intensity of the guided wave controls the propagation wavevector, i.e., the field profile and propagation constant can become power-dependent when one or more of the layered media is characterized by an intensity-dependent refractive index. Two categories of integrated all-optical devices can be anticipated on the basis of these nonlinear optical phenomena.

The first class of optical devices are those in which the nonlinear change in the refractive index is small in comparison to the refractive index difference between the guiding media. In this case the dependence of the propagation wavevector on the power flow can be evaluated from the coupled mode theory ^{/7-9/} and the guided wave field distribution (i.e., field profile) can be approximated by linear guided modes. Devices which have been proposed and operate in this regime include the nonlinear distributed couplers such as gratings and prisms ^{/10-11/} and the nonlinear coherent coupler ^{/12-13/}.

The second category of nonlinear optical devices are those in which the optically induced refractive index-change is comparable with or larger than the index differences between the guiding media. In this case both propagation wavevector and field distribution are power-dependent and this dependence can be evaluated from a more



exact approach in which the nonlinear wave equation is solved subject to continuity of tangential electric and magnetic fields across all the interfaces. Devices which have been proposed in this regime of operation include the nonlinear guided wave optical limiters, lower power threshold devices and optical switching devices /14/. Analytical solutions for the optical fields in Kerr-law media were found by Litvak and Mironov /15/, Miyasi and Nishida /16/, Kaplan /17/ and have been seminal to much of the progress in the field of nonlinear guided waves.

The unique features of nonlinear guided waves in planar layered structures displaying both self-focusing and self-defocusing Kerr-type nonlinearities have been studied intensively in the last years /18-39/.

Langbein, Lederer and Ponath /40/ have developed a formalism that is capable of dealing with arbitrary lossless optical nonlinearities (non-Kerr-like nonlinearities) and authors of the works /41-42/ have applied this technique which does not require analytical field solutions to the nonlinear wave equation in order to evaluate the power dependence of the propagation wavevector /29/ to a variety of planar layered structures.

The question of stability or instability to propagation of various TE_m nonlinear stationary wave solution has been studied by numerical techniques /43-50/.

Wright, Stegeman, Seaton and Moloney /51/ studied Gaussian beam excitation of TE_0 nonlinear guided waves using the beam propagation method. These authors have shown that for a thin dielectric film bounded by two self-focusing media, three different field distributions corresponding to the same guided wave flux level can be excited independently by suitable Gaussian input beams. The problem of multisoliton emission from a nonlinear waveguide was considered by Wright, Stegeman, Seaton, Moloney and Boardman /52/. These authors have demonstrated numerically that external excitation of nonlinear waveguide where the film and substrate are linear but the cladding displays a nonlinear refractive index (optical Kerr effect) can produce sequential threshold behaviour via multisoliton emission from the waveguide. This behaviour is similar to that predicted to occur at a nonlinear interface /53-54/.

The effects of linear absorption on the propagation of TE_0 nonlinear guided waves in an optical waveguide with a nonlinear Kerr-law cladding have also been investigated using the beam propagation method /55/.

Only few experiments dealing with nonlinear guided waves have been reported to date /56-57/. These authors used a single nonlinear self-focusing medium (liquid crystal MBBA or CS_2) bounding a deposited dielectric film. These experiments can be interpreted in terms of nonlinear guided waves with flux dependent field distributions.

The aim of the article is not to give a review of all the papers on nonlinear guided waves, but to select a few topics which illustrate in the simplest way the main physical principles of nonlinear guided waves in layered planar structures and related phenomena. Our selection is dictated by the general criterium of maximum simplicity and for all the points which are not discussed in this paper we advise the reader to consult the recent review /58/. In the present review we analyze in detail nonlinear TE-polarized waves guided by layered planar structures for which the exact stationary solutions of nonlinear wave equation are available.

The paper is organized as follows. Section 2 is devoted to the study of electromagnetic waves guided by nonlinear interfaces. There we discuss the basic concepts and the method used to analyze nonlinear guided wave phenomena. The nonlinear TE-polarized waves guided by thin dielectric films are studied in detail in Section 3. In Section 4 we show that nonlinear TE-polarized waves can also be guided by very thin metal films (nonlinear surface plasmon polaritons). In the last section we briefly present our conclusions.

2. Nonlinear Electromagnetic Waves Guided by a Single Interface

2.1. Intensity-dependent refractive index and dielectric tensor

In the last few years new developments in nonlinear optics have been centered on third-order nonlinear guided-wave interactions which involve the mixing of three optical fields. The nonlinear polarization vector of an optically nonlinear medium is

$$P_i^{NL}(\omega) = \epsilon_0 \chi_{ijk}^{(3)} E_j(\omega) E_k^*(\omega) E_l(\omega), \quad (2.1)$$

where $i = x, y, z$, $\chi^{(3)}$ is the third-order susceptibility and \vec{E} is the total electric field. Note that it is necessary to take the conjugate of one of the mixing optical fields so that the signal output is at the same frequency as the signal input, a prime requisite for all optical signal processing systems operating at a single frequency ω .

If the optical field associated with a plane or a guided wave is large enough, it can change the refractive index of the medium.

For a plane wave in an isotropic material the Fourier component of the polarization field at the frequency ω is:

$$P_i(\omega) = \epsilon_0 [\chi_{ii}^{(1)} + 3\chi_{eff}^{(3)} |E_j(\omega)|^2] E_i(\omega), \quad (2.2)$$

where $\chi_{ii}^{(1)} = n_0^2 - 1$ and n_0 is the linear part of the refractive index. Expressing $|E_j(\omega)|^2$ in terms of the local intensity $I = \frac{1}{2} c \epsilon_0 n_0 |E_j(\omega)|^2$, the intensity-dependent refractive index can be expressed in the form:

$$n = n_0 + n_{2I} I, \quad n_{2I} = \frac{3\chi_{eff}^{(3)}}{c\epsilon_0 n_0}, \quad (2.3)$$

where $n_{2I} > 0$ for self-focusing Kerr-like nonlinearities and $n_{2I} < 0$ for self-defocusing Kerr-like nonlinearities.

For guided waves propagating along the x -axis with z normal to the surfaces, the electric field is written as:

$$E_i = \frac{1}{2} E_i(z) \exp[i(\beta k_0 x - \omega t)] + c.c., \quad (2.4)$$

where β is the effective guided wave index and $k_0 = \omega/c$ is the vacuum wave vector. The expression for the nonlinear polarization vector of an isotropic medium is (see, e.g. /9,59/):

$$P_i^{NL}(z) = c\epsilon_0^2 n_0^2 n_{2I} \left[\frac{2}{3} E_i(z) \sum_j E_j(z) E_j^*(z) + \frac{1}{3} E_i^*(z) \sum_j E_j(z) E_j(z) \right]. \quad (2.5)$$

For TE-polarized waves propagating along the x -axis the electric and magnetic fields are $\vec{E} = (0, E_y, 0)$ and $\vec{H} = (H_x, 0, H_z)$ so that the only nonzero component of the nonlinear polarization vector is

$$P_y^{NL}(z) = c\epsilon_0^2 n_0^2 n_{2I} |E_y(z)|^2 E_y(z). \quad (2.6)$$

In this case only the ϵ_{yy} component of the nonlinear dielectric tensor enters into Maxwell's equations and this will be written as

$$\epsilon_{yy} = n_0^2 + \alpha |E_y|^2, \quad \alpha = c\epsilon_0 n_0^2 n_{2I}. \quad (2.7)$$

The Maxwell's equations are:

$$\frac{dE_y}{dz} = -i\omega\mu_0 H_x, \quad \beta k_0 E_y = \omega\mu_0 H_z \quad (2.8)$$

$$\frac{dH_x}{dz} - i\beta k_0 H_z = i\omega\epsilon_0 \epsilon_{yy} E_y \quad (2.9)$$

where ϵ_{yy} is given by eq. (2.7).

Equations (2.8) and (2.9) give the following nonlinear wave equation for the amplitude function $E_y(z)$:

$$\frac{d^2 E_y}{dz^2} - k_0^2 (\beta^2 - n_0^2) E_y + \alpha k_0^2 |E_y|^2 E_y = 0. \quad (2.10)$$

For real electric fields, eq. (2.10) has an analytical solution /15-17/. This exact solution will be analyzed in detail in the next section.

2.2. Transverse electric polarized nonlinear surface-guided waves

TE-polarized electromagnetic waves cannot be guided by the interface between two dielectric media whose refractive indices do not depend on the intensity. However, when at least one of the two dielectric media exhibits a power-dependent refractive index, a surface-guided wave can exist /15,18,20,60/. In this case the self-focusing optical nonlinearity is not regarded as being small and gives rise to new types of waves that have no counterpart in the linear optics of surface and guided waves (a certain critical power level must be reached before a nonlinear surface guided wave and hence a self-focused channel is created).

We consider a nonlinear interface between an optically linear semi-infinite dielectric medium (called the substrate) with dielectric constant ϵ_s in the region I ($z < 0$) and a semi-infinite Kerr-law nonlinear medium (called the cladding) with the dielectric function $\epsilon = \epsilon_c + \alpha_c |E|^2$ in the region II ($z > 0$).

The TE-polarized wave propagates along the x -axis with the z -axis normal to the surfaces. The only nonvanishing component of the electric field is written as

$$E_y(x, z, t) = \frac{1}{2} E_y(x, z) \exp[i(\beta k_0 x - \omega t)] + c.c., \quad (2.11)$$

where $k = \beta k_0$ is the guided wave wavevector, k_0 is the vacuum wavevector and β is the effective index.

The nonlinear Maxwell's equations for the x -independent guided wave fields (stationary field distribution) are:

$$\frac{d^2 E_y^I}{dz^2} - k_0^2 q_s^2 E_y^I = 0, \quad z < 0 \quad (2.12)$$

$$\frac{d^2 E_y^{II}}{dz^2} - k_0^2 q_c^2 E_y^{II} + \alpha_c k_0^2 (E_y^{II})^3 = 0, \quad z > 0, \quad (2.13)$$

where $q_s^2 = \beta^2 - \epsilon_s$, $q_c^2 = \beta^2 - \epsilon_c$, $\alpha_c = c\epsilon_0 n_0^2 n_{2c}$.

For waves guided by a single interface that are characterized by $E_y(z) \rightarrow 0$ as $|z| \rightarrow \infty$, i.e., the fields decay exponentially away from the boundary: the solutions of eqs. (2.12) and (2.13) are well-known [15-17,61].

$$E_y^I(z) = E_0 \exp(k_0 q_s z), \quad z < 0 \quad (2.14)$$

$$E_y^{II}(z) = \left(\frac{2}{\alpha_c}\right)^{1/2} q_c \left\{ \operatorname{ch} [k_0 q_c (z - z_c)] \right\}^{-1}, \quad z > 0, \quad (2.15)$$

where $q_s = (\beta^2 - \epsilon_s)^{1/2}$, $q_c = (\beta^2 - \epsilon_c)^{1/2}$ and $\alpha_c > 0$ (self-focusing nonlinearity).

For TE-polarized waves both the field E_y and its derivative dE_y/dz is continuous across the interface $z=0$ between nonlinear and linear media. This leads directly to the eigenvalue equation:

$$\epsilon_s = \epsilon_c + \frac{1}{2} \alpha_c E_0^2, \quad (2.16)$$

where E_0 is the surface field. We see from eq.(2.16) that the field amplitude is fixed at the boundary because ϵ_s and ϵ_c are constants and if the limit $\alpha_c \rightarrow 0$ is taken in eq. (2.16), then $E_0 \rightarrow +\infty$, i.e., TE-polarized electromagnetic waves do not exist in the linear limit for a single interface.

The guided wave power in watts per meter of wavefront is given in terms of the Poynting vector as:

$$P = \frac{1}{2} \int_{-\infty}^{\infty} \operatorname{Re}(\vec{E} \times \vec{H}^*) \cdot \hat{x} dz = \frac{\beta}{2c\mu_0} \int_{-\infty}^{\infty} E_y^2(z) dz. \quad (2.17)$$

For Kerr-law media this expression can be evaluated analytically [18]

$$P(\beta) = P_0 \beta \left[\frac{\epsilon_s - \epsilon_c}{q_s} + 2(q_s + q_c) \right]. \quad (2.18)$$

where $P_0 = (\epsilon_0/\mu_0)^{1/2} (2\alpha_c k_0)^{-1}$.

The β -power formula (2.18) can be viewed as the nonlinear dispersion equation $\omega = \omega(\kappa, P)$, i.e., the frequency (ω) wave number (κ) relationship for a given power level.

It is possible to evaluate the nonlinear guided wave attenuation coefficient approximately from the imaginary component of the dielectric constant by assuming that the field distribution obtained in the lossless case will still be valid if the loss per wavelength is small [60,62,63].

A new formalism that is capable of dealing with arbitrary local lossless nonlinearities have been developed by Langbein, Lederer and Ponath [40]. This technique does not require analytical field solutions to the nonlinear wave equation in order to evaluate the flux dependence of the propagation wavevector.

As is well known the form of the dielectric function is determined by the physical processes which lead to the nonlinearity. The Kerr nonlinearity which is quadratic in the local optical fields $\epsilon^{NL} = \alpha |\vec{E}|^2$ arises from electronic nonlinearities, thermal effects, etc. The dependence of the dielectric function on the electric field is not quadratic in semiconductor materials where the nonlinearities are due to absorption leading to the creation of excitons, plasmons, etc. In this case the optical nonlinearity is of the form $\epsilon^{NL} = \alpha_r |\vec{E}|^r$, where $1 < r < 2$ [64-67]. Furthermore, in realistic materials, it is not possible to optically change the refractive index indefinitely and saturation effect sets in. The values of the saturated change Δn_{sat} of the refractive index varies from 10^{-1} to 10^{-4} . For nonlinear interface the saturation effect is important because the interesting flux-dependent surface-guided wave properties occur when the optically induced change in the refractive index Δn_{sat} is comparable to or larger than the refractive index difference $n_s - n_c$ which exists at low powers between the substrate and the cladding.

We model the dielectric function of the nonlinear self-focusing ($\alpha_c > 0$) cladding as in [41,42,60,68]:

$$\epsilon_{xx} = \epsilon_{yy} = \epsilon_{zz} = \epsilon_c + \epsilon_{sat} \left[1 - \exp\left(-\frac{\alpha_c E_y^2}{\epsilon_{sat}}\right) \right] \quad (2.19)$$

$$\epsilon_{xx} = \epsilon_{yy} = \epsilon_{zz} = \epsilon_c + \frac{\alpha_c E_y^2}{\left(1 + \frac{\alpha_c E_y^2}{\epsilon_{sat}}\right)} \quad (2.20)$$

$$\epsilon_{xx} = \epsilon_{yy} = \epsilon_{zz} = \epsilon_c + \alpha_{c,r} E_y^r, \quad r \geq 1. \quad (2.21)$$

Note that for both dielectric tensors (2.19) and (2.20) the maximum change in the dielectric function is ϵ_{sat} , that is, for $|\vec{E}|^2 \rightarrow \infty$, $\epsilon \rightarrow \epsilon_c + \epsilon_{sat}$. For small fields $\epsilon \rightarrow \epsilon_c + \alpha_c E_y^2$, i.e., the usual Kerr-law medium case. The dielectric tensors (2.19), (2.20) and (2.21) can be written in the general form as:

$$\epsilon_{xx} = \epsilon_{yy} = \epsilon_{zz} = \epsilon_c + \epsilon_c^{NL} (E_y^2). \quad (2.22)$$

The nonlinear wave equation for the real quantity (in the absence of loss) $E_y(z)$ is:

$$\frac{d^2 E_y}{dz^2} + k_0^2 [\epsilon_c + \epsilon_c^{NL} (E_y^2) - \beta^2] E_y = 0. \quad (2.23)$$

For surface-guided waves characterized by $E_y(z) \rightarrow 0$ as $|z| \rightarrow \infty$ the first integral of eq. (2.23) can be written as:

$$\left(\frac{dE_y}{dz}\right)^2 = \Phi_c(E_y, \beta) = k_0^2 \left[q_c^2 E_y^2 - \int_0^{E_y^2} \epsilon_c^{NL}(E_y^2) d(E_y^2) \right]. \quad (2.24)$$

The continuity of E_y and dE_y/dz across the nonlinear boundary $z=0$ between the linear substrate and the nonlinear cladding leads to the dispersion relation

$$q_s + \bar{q}_c = 0 \quad (2.25)$$

$$\bar{q}_c = (-1)^{M_c} (\beta^2 - \epsilon_{cNL})^{1/2} \quad (2.26)$$

$$\epsilon_{cNL} = \epsilon_c + \frac{1}{E_0^2} \int_0^{E_0^2} \epsilon_c^{NL}(E_y^2) d(E_y^2), \quad (2.27)$$

where E_0 is the surface field, ϵ_{cNL} is an averaged dielectric function of the nonlinear medium, $M_c=1$ if a self-focused peak occurs in the nonlinear cladding and $M_c=0$ if there is no field maximum in the nonlinear medium.

In our case of a self-focusing nonlinear cladding ($\alpha_c > 0$) a self-focused field maximum occurs in that medium ($M_c=1$) and the dispersion relation (eigenvalue equation) (2.25) becomes:

$$\epsilon_s = \epsilon_c + \frac{1}{E_0^2} \int_0^{E_0^2} \epsilon_c^{NL}(E_y^2) d(E_y^2) \quad (2.28)$$

from which the surface field E_0 can be determined. For a Kerr-law nonlinear cladding the eigenvalue equation (2.28) reduces to eq. (2.16). From eq. (2.28) we obtain the important result that TE-polarized surface guided waves can be supported by a single nonlinear interface if and only if $\epsilon_s > \epsilon_c$.

The guided wave power flow parallel to the interface is $P = P_s + P_c$, where P_c has the expression ^{140/}:

$$P_c = \frac{\beta}{2\mu_0 c} \left[\int_0^{\bar{E}_y} \frac{E_y^2 dE_y}{\Phi_c^{1/2}} + (-1)^{M_c} \int_{\bar{E}_y}^{E_0} \frac{E_y^2 dE_y}{\Phi_c^{1/2}} \right]. \quad (2.29)$$

Here $M_c=1$ (there is a field maximum in the nonlinear cladding), $\Phi_c^{1/2} = dE_y/dz$ and \bar{E}_y is the field maximum evaluated from

$\Phi_c(\bar{E}_y) = 0$. Finally we obtain the following expression for the total power flow $P = P_s + P_c$

$$P_s = \frac{1}{2} P_0 \beta \frac{u}{q_s} \quad (2.30)$$

$$P_c = \frac{1}{2} P_0 \beta \left[\int_0^{\bar{u}} \frac{dx}{[\varphi(x)]^{1/2}} + (-1)^{M_c} \int_{\bar{u}}^u \frac{dx}{[\varphi(x)]^{1/2}} \right], \quad (2.31)$$

where $M_c = 1$.

Here we have

$$\varphi(x) = \beta^2 - \epsilon_c - \epsilon_{sat} + \frac{\epsilon_{sat}^2}{x} \left[1 - \exp\left(-\frac{x}{\epsilon_{sat}}\right) \right] \quad (2.32)$$

$$\varphi(x) = \beta^2 - \epsilon_c - \epsilon_{sat} + \frac{\epsilon_{sat}^2}{x} \ln\left(1 + \frac{x}{\epsilon_{sat}}\right) \quad (2.33)$$

$$\varphi(x) = \beta^2 - \epsilon_c - \frac{2}{(r+2)} x^{r/2} \quad (2.34)$$

which correspond to the dielectric tensors (2.19), (2.20) and (2.21), respectively; $u = \alpha_c E_0^2$ is obtained from the eigenvalue equation (2.28) and \bar{u} is determined from $\varphi(\bar{u}) = 0$.

For Kerr-law media we have $\varphi(x) = \beta^2 - \epsilon_c - \frac{1}{2} x$ and the integrals in (2.31) can be evaluated analytically:

$$P_c = 2 P_0 \beta \left[(\beta^2 - \epsilon_c)^{1/2} + (\beta^2 - \epsilon_c - \frac{1}{2} u)^{1/2} \right], \quad (2.35)$$

where $u = \alpha_c E_0^2 = 2(\epsilon_s - \epsilon_c)$ is obtained from the eigenvalue equation (2.16).

In the case of a saturable nonlinear cladding characterized by the dielectric functions (2.19) and (2.20) there is a maximum in the change $\Delta\epsilon_c$ of the dielectric constant which can be induced optically, i.e., $\epsilon \rightarrow \epsilon_c + \epsilon_{sat}$ for large fields ($|\vec{E}| \rightarrow \infty$). Thus the effective index β approaches its limiting value of $(\epsilon_c + \epsilon_{sat})^{1/2}$ asymptotically with increasing power. A necessary condition for the existence of solution of the eigenvalue (2.28) in the unknown E_0 is $\epsilon_s < \epsilon_c + \epsilon_{sat}$. From the condition that $\Phi_c(\bar{E}_y) = 0$ we thus obtain that $\beta^2 < \epsilon_c + \epsilon_{sat}$, therefore the permitted β -region for nonlinear surface-guided wave is $\epsilon_s^{1/2} < \beta < (\epsilon_c + \epsilon_{sat})^{1/2}$.

For a power-law cladding ($r \neq 2$) we have:

$$u = \left[\frac{(r+2)(\epsilon_s - \epsilon_c)}{2} \right]^{2/r} \quad (2.36)$$

$$\bar{u} = \left[\frac{(r+2)(\beta^2 - \epsilon_c)}{2} \right]^{2/r} \quad (2.37)$$

and the power flow P_s, P_c are given by eq. (2.30) and (2.31) with P_0 replaced by $P_{0,r} = (\epsilon_0/\mu_0)^{1/2} (2\kappa_0 \alpha_{c,r}^{2/\nu})^{-1}$.

The numerical results for TE-polarized surface guided waves are shown in Fig. 1 for Kerr-law claddings ($\nu = 2$), powerlaw claddings ($\nu \neq 2$) and saturable claddings.

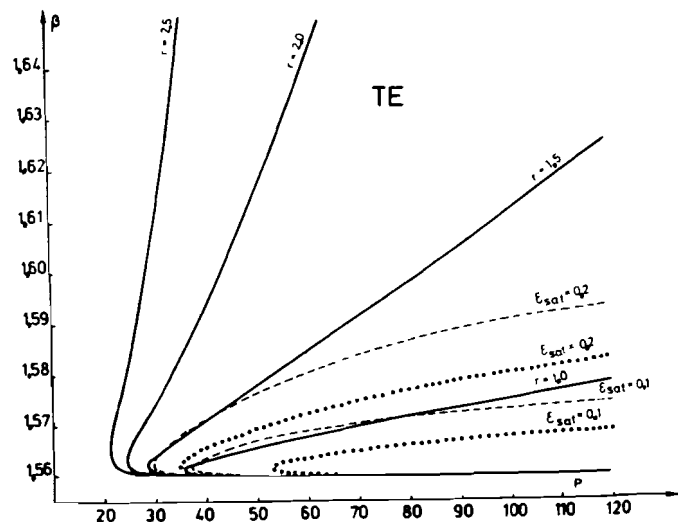


Fig. 1. The dependence of the effective index β on the power flow for TE waves guided by the interface between a self-focusing cladding ($n_c = 1.55, n_{2c} = 10^{-9} \text{ m}^2/\text{W}$) and a linear substrate ($n_s = 1.56$). The dashed and dotted lines correspond to the dielectric functions (2.19) and (2.20), respectively (after /69/.)

The dependence of the power flux P on the effective index β was evaluated for a nonlinear cladding characterized by $n_c = 1.55, n_{2c} = 10^{-9} \text{ m}^2/\text{W}$ (liquid crystal MBBA) at $\lambda = 0.515 \mu\text{m}$ (argon ion laser) in contact with a linear substrate with $n_s = 1.56$. The values of the nonlinear coefficients $\alpha_{c,r}$ were chosen to produce equal minimum values of the power flux: $\alpha_{c,1} = 4.7 \times 10^{-7} \text{ m/V}, \alpha_{c,1.5} = 1.75 \times 10^{-9} (\text{m/V})^{1.5}, \alpha_{c,2.5} = 2.3 \times 10^{-14} (\text{m/V})^{2.5}$ (see /69/).

We see from Fig. 1 that the minimum power required for the excitation of nonlinear TE-polarized surface guided waves increases with decreasing ϵ_{sat} .

2.3. Stability to propagation of nonlinear single-interface guided waves

The reflection of a plane wave from an interface between a linear medium and a nonlinear medium was apparently studied first in /70,17/. Following this pioneering works there have been several theoretical /53,54,71/ and experimental /72/ studies of the interaction of Gaussian light beams with a nonlinear interface. Numerical techniques have been used by Akhmediev, Korneev and Kuzmenko /43/ to study the excitation of nonlinear surface waves by Gaussian light beams. The question of stability to propagation of nonlinear surface-guided waves is crucial to the problem of the excitation of these waves by external sources. It was found in /43/ that both stable and unstable nonlinear surface waves can be excited by Gaussian light beams incident on the nonlinear interface at grazing angles.

Consider the nonlinear interface between a linear substrate with dielectric constant ϵ_s in the region I ($z < 0$) and a nonlinear Kerr-law cladding with dielectric function $\epsilon = \epsilon_c + \alpha_c |\vec{E}|^2$ in the region II ($z > 0$). The TE-polarized wave of frequency ω propagates along the x axis and the only nonvanishing component of the electric field E_y is homogeneous in y direction (z being the transverse coordinate). The parabolic equation for the slowly varying amplitude $A(x,z) = \alpha_c^{-1/2} E_y(x,z)$ is then

$$-2i\beta\kappa_0 \frac{\partial A}{\partial x} = \frac{\partial^2 A}{\partial z^2} - \gamma^2(z)\kappa_0^2 A + \Theta(z)\kappa_0^2 |A|^2 A. \quad (2.38)$$

Here $\Theta(z) = 0$ for $z < 0$ and $\Theta(z) = 1$ for $z > 0$, $\gamma^2(z) = \beta^2 - n_s^2$ for $z < 0$ and $\gamma^2(z) = \beta^2 - n_c^2$ for $z > 0$. Note that the usual stationary solution of eq. (2.38), i.e., $A(0,z) = A_c(z)$ can be obtained analytically (see eqs. (2.14) and (2.15)).

Equation (2.38) has two integrals of motion:

$$I(\beta) = \kappa_0 \int_{-\infty}^{\infty} |A|^2 dz = (P_0 \beta)^{-1} P(\beta) \quad (2.39)$$

$$H(\beta) = \kappa_0 \int_{-\infty}^{\infty} \left[\left| \frac{\partial A}{\partial z} \right|^2 + \kappa_0^2 \gamma^2(z) |A|^2 - \frac{1}{2} \kappa_0^2 \Theta(z) |A|^4 \right] dz \quad (2.40)$$

and for arbitrary solutions of eq. (2.38) we thus have $dI/dx = 0$ and $dH/dx = 0$. Note that eq. (2.38) is a mixed-type linear/nonlinear Schrödinger-like equation with coefficients which depend on the transverse coordinate z . The absence of translational symmetry along the z axis means that we cannot use the elegant apparatus of the inverse scattering method /73,74/ to solve analytically the problem.

To avoid numerical stability question we selected for the difference approximation of eq. (2.38) the Crank-Nicolson scheme^{/75,76/}. We have chosen the grid sizes equal in magnitude $\kappa_0 \Delta x = \kappa_0 \Delta z = 0.4$. The corresponding system of nonlinear equations was solved by Newton-Picard method (see^{/75/}). We have found that two iterations for the Newton-Picard method are enough in practice. This difference scheme makes it possible to conserve the integrals of motion (2.39) and (2.40) on the grid. The conservation of the total power flow was always better than 99%. For a Kerr-law nonlinear cladding and for $\beta = 1.5607$ on the negative sloped branch ($dI/d\beta < 0$) of the nonlinear dispersion curve (see Fig. 1) the nonlinear stationary wave is unstable on propagation. In this case the nonlinear surface-guided wave is ejected into the linear substrate as the result of the propagation (see Fig. 2).

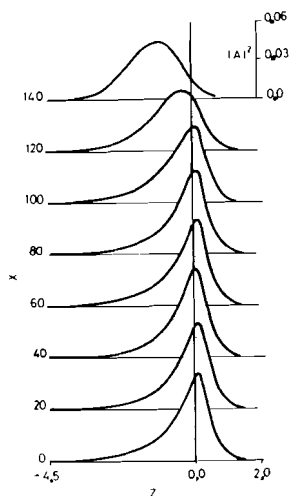


Fig. 2. Evolution of nonlinear surface wave field distribution with propagation distance. Here $n_c = 1.55$, $n_{2c} = 10^{-9} \text{ m}^2/\text{W}$, $n_s = 1.56$ and the initial field pattern $A_0(z)$ corresponds to $\beta = 1.5607$.

The evolution of the nonlinear surface wave field distribution with propagation distance for $\beta = 1.574$ on the positively sloped branch of the nonlinear dispersion curve ($dI/d\beta > 0$) is shown in

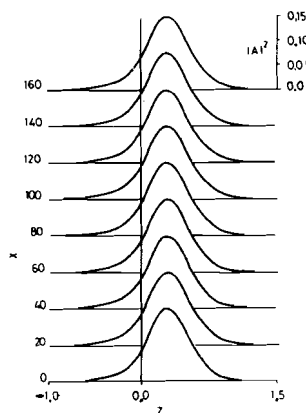


Fig. 3. The same as in Fig. 2, but for $\beta = 1.574$.

Fig. 3. For this value of the propagation constant the nonlinear stationary wave $A_0(z)$ is stable on propagation over at least 300 wavelengths. To conclude this section we point out that for the related problem of self-focusing of plane waves in infinite media Kolokolov^{/77/} has shown that the solutions are stable for $dI/d\beta > 0$. The numerical results presented here for TE-polarized waves guided by a nonlinear interface yield the same stability criterion, i.e., $dI/d\beta > 0$.

2.4. Transverse magnetic polarized guided waves at a nonlinear interface

Surface polaritons are electromagnetic waves guided by a single interface between two semi-infinite media, or by a single or multiple films bounded by two semi-infinite media (see^{/78,79/}). In all cases the electromagnetic fields decay with distance from the boundary into the semi-infinite media in an exponential-like fashion, resulting in fields localized near or at the surface. In the case of transverse magnetic (TM) polarization the magnetic vector is oriented perpendicular to the plane of incidence, i.e., the plane defined by the direction of propagation and the normal to the surface.

Consider one of the simplest case, namely that of electromagnetic waves guided by a single interface between two semi-infinite linear media. The dielectric constants are ϵ_c and ϵ_s where the subscripts c and s refer to the cladding and the substrate. In the linear case only TM-polarized surface polaritons can be supported by a single interface and only if $\epsilon_c > 0$, $\epsilon_s < 0$ and $\epsilon_c < |\epsilon_s|$. The effective index $\beta = \kappa/\kappa_0$, where κ is the propagation wavevector and $\kappa_0 = \omega/c$ is given by (see^{/79/}):

$$\beta^2 = \frac{\epsilon_s \epsilon_c}{\epsilon_s + \epsilon_c} = \frac{|\epsilon_s| \epsilon_c}{(|\epsilon_s| - \epsilon_c)} \quad (2.41)$$

In the following we consider the effects of optical nonlinearities on surface and guided electromagnetic waves in which these nonlinearities are not regarded as small and give rise to new types of waves that in some cases have no counterpart in the linear optics of surface and guided waves. Note that the propagation of nonlinear TM-polarized surface waves at a plasma boundary was apparently studied first by Alanakyan^{/80/}. For the TM-polarization and Kerr-like media there were two approximations frequently used in the literature: a) the uniaxial $\epsilon_{xx}(|E_x|^k)$ approximation, in which the component of the dielectric tensor, parallel to the surface, ϵ_{xx} depends on the field component, parallel to the surface, E_x ^{/19/} and b) the un-

iaxial $\epsilon_{zz} (|E_z|^2)$ approximation, in which the component of the dielectric tensor, perpendicular to the surface, ϵ_{zz} depends on the normal field component E_z ^{/81/}.

The dispersion relation of TM-polarized nonlinear surface polaritons guided by the interface between a linear dielectric and a nonlinear Kerr-law dielectric medium in the uniaxial $\epsilon_{xx} (|E_x|^2)$ approximation:

$$\begin{aligned} \epsilon_{xx} &= \epsilon_x + \alpha_{xx} |E_x|^2 \\ \epsilon_{zz} &= \epsilon_z \end{aligned} \quad (2.42)$$

was studied in detail in ^{/19/}. In this approximation, and in the case $\epsilon_x > 0$, $\epsilon_z > 0$ dispersion curves of TM-polarized nonlinear surface polaritons at a quartz-vacuum interface were plotted ^{/60/}. Exact dispersion relation of nonlinear TM-polarized waves at the boundary between two semi-infinite nonlinear uniaxial media characterized by diagonal dielectric tensors of the type (2.42) has been derived by Lomtev ^{/21/} and Yu ^{/27/}. The influence of oscillations in the transition layer on TM-polarized nonlinear surface polariton spectra has been first discussed in ^{/82/} in the case of uniaxial $\epsilon_{xx} (|E_x|^2)$ approximation and subsequently in ^{/83/} for the uniaxial $\epsilon_{zz} (|E_z|^2)$ approximation:

$$\begin{aligned} \epsilon_{xx} &= \epsilon_x \\ \epsilon_{zz} &= \epsilon_z + \alpha_{zz} |E_z|^2. \end{aligned} \quad (2.43)$$

For TM-waves in Kerr-law media and in the case of uniaxial $\epsilon_{xx} (|E_x|^2)$ approximation, the differential equation for $E_x(z)$ field component is:

$$\frac{d^2 E_x}{dz^2} - \kappa_0^2 q_s^2 E_x - \frac{\kappa_0^2 q_s^2 \alpha_x}{\epsilon_x} E_x^3 = 0, \quad (2.44)$$

where $s=f, c$, refers to the substrate, film and cladding, respectively. This equation has analytical solutions ^{/19/}. For example, if $\alpha_c < 0$ and $\alpha_s < 0$ we have

$$E_x(z) = \left(\frac{2\epsilon_s}{\kappa_s} \right)^{1/2} \left\{ \text{ch} [k_0 q_s (z_s - z)] \right\}^{-1}, \quad z < 0 \quad (2.45)$$

$$E_x(z) = \left(\frac{2\epsilon_c}{|\alpha_c|} \right)^{1/2} \left\{ \text{ch} [k_0 q_c (z_c + z)] \right\}^{-1}, \quad z > 0. \quad (2.46)$$

If $\alpha_c > 0$ and $\alpha_s > 0$ then ch is replaced by sh . Note that, because the sign of the term proportional to α_s in eq. (2.44) is now negative, versus positive for the TE polarized case, the field distributions differ between TE and TM-polarized $\epsilon_{xx} (|E_x|^2)$ cases.

An alternative approach is to eliminate $E_x(z)$ and $E_z(z)$ from Maxwell's equations and to obtain a single equation for the remaining field $H_y(z)$. In the uniaxial $\epsilon_{zz} (|E_z|^2)$ approximation we have:

$$\frac{d^2 H_y}{dz^2} - \kappa_0^2 q_s^2 H_y + \frac{\kappa_0^2 \beta^4 \alpha_y}{c^2 \epsilon_0^2 \epsilon_{zz}^3} H_y^3 = 0. \quad (2.47)$$

This differential equation is not exactly solvable because of the ϵ_{zz}^3 term in the denominator. We note that for most materials the quantity $\beta \epsilon = |\alpha_y \epsilon_z^2|$ is smaller than 0.01 and in some exceptional cases, e.g., InSb, it can reach 0.1. The approximation $\epsilon_{zz} \approx \epsilon_y$ in the denominator of the third term in eq. (2.47) implies only a small error in an already small term. In this limit the solutions for $H_y(z)$ now have exactly the same form as for the exactly solvable TE-case with α_s replaced by $\alpha_s' = \beta^4 (c^2 \epsilon_0^2 \epsilon_y^3)^{-1} \alpha_s$. Because of these similarities the uniaxial $\epsilon_{zz} (|E_z|^2)$ approximation leads to similar power dependent behaviour for both TE and TM-polarized guided waves.

TM-polarized electromagnetic waves guided by a single interface were investigated in detail in ^{/63/}. Both $\epsilon_{xx} (|E_x|^2)$ and $\epsilon_{zz} (|E_z|^2)$ approximations for TM-waves were analyzed and the guided wave wavevector and the attenuation coefficient versus guided wave power were evaluated for a variety of material conditions. The nonlinear guided wave attenuation coefficient was calculated approximately from the imaginary components of the dielectric constants ϵ_{sI} and ϵ_{cI} . Assuming small losses it can be easily shown that

$$\beta_I = \frac{1}{2\beta_R \rho} (\epsilon_{sI} P_s + \epsilon_{cI} P_c), \quad (2.48)$$

where β_I and β_R are the imaginary and the real part of the effective index β ^{/63/}. Akhmediev ^{/84/} has given a theory of nonlinear surface TM-waves, but the analysis was restricted to isotropic nonlinear media in which the two electric field components have equal weight in the dielectric constant. Boardman, Maradudin, Stegeman, Twardowski and Wright ^{/85/} presented a numerical method for solving Maxwell equations for TM waves at a nonlinear interface which is applicable to arbitrary forms of dispersive nonlinearity. They did this by transforming the infinite transverse plane into a finite interval and making use of the asymptotic boundary conditions.

In the following we derive exact dispersion relation of TM polarized guided waves at an interface between either a linear dielectric or metal and a nonlinear Kerr-law dielectric [39]. This dispersion relation is a polynomial equation involving the boundary values of the electric field components, the medium parameters and the guided wave effective index β . Note that surface electromagnetic waves guided by the boundary between a nonlinear dielectric and a metal are of particular interest since they correspond to the only type of nonlinear single-interface wave that does not have a power threshold.

As is well known, TM-polarized waves exhibit two electric field components, one parallel (E_x) to the wave vector and one perpendicular (E_z) to the surfaces. To define the effects of an intensity-dependent refractive index, it is necessary to first examine the nonlinear polarization field. The electric field vector is

$$\vec{E}(\vec{r}, t) = \frac{1}{2} [E_x(z)\vec{x} + E_z(z)\vec{z}] \exp[i(\beta k_0 x - \omega t)] + c.c., (2.49)$$

where $E_x(z)$ and $E_z(z)$ are $\pi/2$ out of phase with one another, i.e., $|E_z|^2 = E_z^2$ and $|E_x|^2 = -E_x^2$. The nonzero components of the nonlinear polarization vector are (Stegeman [9]):

$$P_x^{NL}(z) = \epsilon_0 (\alpha_{xx} |E_x(z)|^2 + \alpha_{xz} |E_z(z)|^2) E_x(z) (2.50)$$

$$P_z^{NL}(z) = \epsilon_0 (\alpha_{zx} |E_x(z)|^2 + \alpha_{zz} |E_z(z)|^2) E_z(z) (2.51)$$

Thus for a Kerr-law medium the components of the dielectric tensor are

$$\epsilon_{xx} = \epsilon_x + \alpha_{xx} |E_x|^2 + \alpha_{xz} |E_z|^2 (2.52)$$

$$\epsilon_{zz} = \epsilon_z + \alpha_{zx} |E_x|^2 + \alpha_{zz} |E_z|^2, (2.53)$$

where the values of the Kerr-type optical nonlinearities α_{ij} depend on the particular nonlinear mechanism under consideration. For electronic nonlinearities obtained from a power law expansion of the polarization in terms of field products we have $\alpha_{xx} = \alpha_{zz} = 3\alpha_{xz} = -3\alpha_{zx} = c\epsilon_0 n_0^2 n_2$, whereas for electrostrictive nonlinearities $\alpha_{xx} = \alpha_{zz} = \alpha_{xz} = \alpha_{zx} = \alpha_{zx} = c\epsilon_0 n_0^2 n_{2I}$ where $n = n_0 + n_{2I} I$, n_0 is the linear part of the refractive index and n_{2I} is the intensity-dependent refractive index coefficient.

Starting from the Maxwell equations for TM polarized guided waves the electric field components $E_x(z)$ and $E_z(z)$ obey

$$\frac{dE_x}{dz} = -i \frac{k_0}{\beta} (\epsilon_{zz} - \beta^2) E_z (2.54)$$

$$\frac{d}{dz} (\epsilon_{zz} E_z) = -i \beta k_0 \epsilon_{xx} E_x (2.55)$$

$$H_y = -\frac{c\epsilon_0}{\beta} \epsilon_{zz} E_z (2.56)$$

The key point of our analysis is that for guided TM waves, i.e., $E \rightarrow 0$ and $dE/dz \rightarrow 0$ as $z \rightarrow \pm\infty$, eqs. (2.54) and (2.55) have a first integral which can be written as

$$\frac{1}{2} \left(\frac{dE_x}{dz} \right)^2 + U(E_x, E_z) = 0, (2.57)$$

where

$$U(E_x, E_z) = \frac{1}{2} k_0^2 \epsilon_x E_x^2 + \frac{1}{2} k_0^2 (\beta^2 - \epsilon_z) E_z^2 + \frac{1}{2} k_0^2 \alpha_{xz} E_x^2 E_z^2 - \frac{1}{4} k_0^2 \alpha_{xx} (E_x^4 + E_z^4) (2.58)$$

as was first shown by Berkhoer and Zakharov [86].

The solution of Maxwell equations (2.54) and (2.55) in the semi-infinite linear substrate characterized by a dielectric constant ϵ_s (for a dielectric $\epsilon_s > 0$, for a metal $\epsilon_s < 0$) which occupies the lower-half space $z < 0$ can be written as:

$$E_x(z) = E_{ox} \exp(k_0 \gamma_s z), \quad z < 0, (2.59)$$

where $\gamma_s = (\beta^2 - \epsilon_s)^{1/2}$, $E_{ox} = E_x(0)$ and $\beta^2 > \epsilon_s$ for a dielectric. Furthermore, in the nonlinear medium eq. (2.54) can be rearranged as:

$$E_z = \frac{i\beta}{k_0(\epsilon_{zz} - \beta^2)} \frac{dE_x}{dz} (2.60)$$

which gives

$$D_z = \frac{i\beta \epsilon_{zz}}{k_0(\epsilon_{zz} - \beta^2)} \frac{dE_x}{dz}, (2.61)$$

where D_z is the z component of the displacement vector \vec{D} . Equation (2.61) also holds in the linear medium with ϵ_{zz} replaced by ϵ_s . From standard electromagnetic theory D_z and E_x must be continuous across the interface $z=0$. Now we define $E_{oz} = E_z(0)$ and the value ϵ_{nz} of the z component of the dielectric tensor at the interface $z=0$ which depends on the boundary fields:

$$\epsilon_{nz} = \epsilon_z - \alpha_{zx} E_{ox}^2 + \alpha_{zz} E_{oz}^2 (2.62)$$

From the continuity of D_z at the interface $z=0$ we obtain the following relation between the boundary values of the fields:

$$E_{Ox} = \frac{i q_s}{\beta \epsilon_s} (\epsilon_z - \alpha_{zx} E_{Ox}^2 + \alpha_{zz} E_{Oz}^2) E_{Oz}. \quad (2.63)$$

In the limit of weak fields eq. (2.63) reproduces the usual relation between the boundary values of the fields. Furthermore by using the first integral (2.57) we finally obtain the following eigenvalue equation for β [39]:

$$\beta^4 \left[2 \epsilon_s^4 \epsilon_{nl} - \epsilon_x \epsilon_s^2 \epsilon_{nl}^2 - \epsilon_z \epsilon_s^4 - \frac{1}{2} \alpha_{zz} E_{Oz}^2 (\epsilon_s^4 + \epsilon_{nl}^4) - \alpha_{xz} E_{Oz}^2 \epsilon_s^2 \epsilon_{nl}^2 \right] + \beta^2 \left[\epsilon_x \epsilon_s^3 \epsilon_{nl}^2 + \alpha_{zz} E_{Oz}^2 \epsilon_s \epsilon_{nl}^4 + \alpha_{xz} E_{Oz}^2 \epsilon_s^3 \epsilon_{nl}^2 - \epsilon_s^4 \epsilon_{nl}^2 \right] - \frac{1}{2} \alpha_{zz} E_{Oz}^2 \epsilon_s^2 \epsilon_{nl}^4 = 0. \quad (2.64)$$

Note that the particular case of an isotropic nonlinear cladding, i.e., $\epsilon_x = \epsilon_z = \epsilon_c$, $\alpha_{xx} = \alpha_{zz} = \alpha_{xz} = \alpha_{zx} = \alpha_c$ was studied in detail by Akhmediev [84]. In this case the eigenvalue equation for β has a simpler form:

$$\beta^2 = \frac{\epsilon_s \epsilon_{nl}^2 (2 \epsilon_s - \epsilon_{nl} - \epsilon_c)}{\epsilon_s^2 (3 \epsilon_{nl} - \epsilon_c) - \epsilon_{nl}^2 (\epsilon_{nl} + \epsilon_c)}, \quad (2.65)$$

where $\epsilon_{nl} = \epsilon_c + \alpha_c (E_{Oz}^2 - E_{Ox}^2)$ is the value of the dielectric constant of the nonlinear Kerr-law cladding at the interface $z=0$.

Given the material parameters, equations (2.63) and (2.64) allow the boundary values of the electric field components inside the nonlinear medium to be determined as a function of β (at least numerically). Equations (2.54) and (2.55) can then be integrated using the boundary values to give the field distribution in the nonlinear medium. The field distribution in the linear medium is simple exponential (see eq. (2.59)). Once the fields are obtained, the guided wave flux can be calculated by integrating the time-averaged Poynting vector over the depth Z . Finally we have $P = P_s + P_c$, where

$$P_s = \frac{\epsilon_{nl}^2 E_{Oz}^2}{4 \mu_0 \omega \beta q_s \epsilon_s} \quad (2.66)$$

$$P_c = \frac{k_0}{2 \mu_0 \omega \beta} \int_0^\infty \epsilon_{zz}(z) E_z^2(z) dz. \quad (2.67)$$

A first survey of the field patterns and the permitted β -regions can be obtained from the inspection of the so-called "phase trajectories" of the nonlinear surface waves (see [40,84]). Let us consider various particular case for an isotropic nonlinear cladding with $\epsilon_x = \epsilon_z = \epsilon_c$ and $\alpha_{xx} = \alpha_{zz} = \alpha_{xz} = \alpha_{zx} = \alpha_c$.

a) $\epsilon_c > 0$, $\alpha_c > 0$ and $\epsilon_s < 0$.

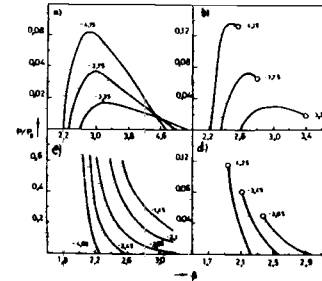


Fig. 4. Dependence of the dimensionless power flow P/P_0 of the surface wave on the effective index β for four different cases. For the medium with positive dielectric constant (ϵ_c or ϵ_s) we choose the value $\epsilon = 2.25$. The values of the dielectric constant of the adjoining medium are indicated above the curves (after [84]).

The dependence of the dimensionless power flow P/P_0 on the effective index β for $\epsilon_c = 2.25$ and several values of ϵ_s is shown in Fig. 4a. It can be seen that by increasing the effective index β , the guided wave power increases up to some limiting value and then decreases to zero. This is related to the fact that, in a medium with negative dielectric constant, the power flow and the wavevector have opposite directions and in some region of β values the power flow is decreasing with increasing effective index β . We note that the magnetic field for this solution attains its maximum at the interface between two media. In this case the effective index for the nonlinear surface wave is greater than the value $\beta_l = [\epsilon_c |\epsilon_s| (|\epsilon_s| - \epsilon_c)^{-1}]^{1/2}$, corresponding to a TM-polarized linear surface polariton.

b) $\epsilon_c < 0$, $\alpha_c > 0$ and $\epsilon_s > 0$.

Fig. 4b shows the dependence of the dimensionless power flow P/P_0 on the propagation constant β for $\epsilon_s = 2.25$ and several values of ϵ_c . In the present case the surface wave exist in a bounded range of variation of β and the effective index is greater than the value $\beta_l = [|\epsilon_c| \epsilon_s (|\epsilon_c| - \epsilon_s)^{-1}]^{1/2}$. Let us note that as in the case a) there is a maximum power which can be transmitted.

c) $\epsilon_c < 0$, $\alpha_c < 0$ and $\epsilon_s > 0$.

For the present case Fig. 4c shows the β -dependence of the dimensionless power flow P/P_0 . We see that for $\beta = \beta_l$ the power flow is equal to zero and increases the infinity as β approaches

$n_s = \epsilon_s^{1/2}$. We remind that in the case that $\epsilon_s > |\epsilon_c|$ TM-polarized linear surface polaritons do not exist. As we can see from Fig. 4c, TM-polarized nonlinear surface polaritons can exist in the case $\epsilon_s > |\epsilon_c|$ when the power flow exceeds some threshold value (the curves for $\epsilon_c = -2.1$ and $\epsilon_c = -1.45$).

d) $\epsilon_c > 0$, $\alpha_c < 0$, $\epsilon_s < 0$.

Figure 4d shows the β -dependence of the dimensionless power flow P/P_0 for $\epsilon_c = 2.25$ and several values of ϵ_s . Thus for negative nonlinearity, i.e., the cases c) and d), as the power flow increases, the effective index β decreases from the value $\beta = \beta_l$ corresponding to the TM-polarized linear surface polaritons.

e) $\epsilon_c > 0$, $\alpha_c > 0$, $\epsilon_s > 0$.

In this case the "phase-path diagram" and the field pattern show that the magnetic field attains its maximum in the self-focusing nonlinear cladding ($\alpha_c > 0$) and not at the interface $z = 0$. This nonlinear wave can be guided by the interface between a self-focusing dielectric cladding and a linear dielectric substrate, provided that the power threshold is exceeded and in this sense is similar to TE-polarized surface polaritons at a nonlinear interface (see /18,20,60/).

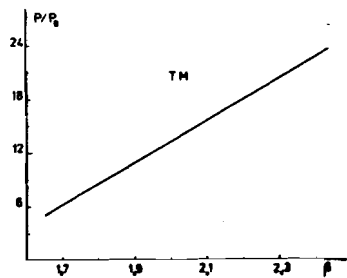


Fig. 5. Dependence of the energy flux P/P_0 of a surface wave on the effective refractive index β in the case when $\epsilon_c = 2.25$, $\epsilon_s = 2.5$ and $\alpha_c > 0$ (after /84/).

transverse distribution of the electric field component E_x for the electronic nonlinearity and for several values of the propagation constant β . Note that for both electronic and electrostrictive self-focusing nonlinearities there is a maximum power which can be transmitted and the effective index β is greater than the value β_l corresponding to a TM-polarized linear surface wave.

For the present case Fig. 5 shows the β -dependence of the dimensionless power flow P/P_0 for $\epsilon_c = 2.25$ and $\epsilon_s = 2.5$. This TM-polarized wave has no analogue in the linear optics of surface-guided waves /84/.

In fig. 6 we present the β -dependence of the power flow P for the nonlinear self-focusing dielectric-metal interface for both electronic, $\alpha_{xx} = 3\alpha_{xz}$ (curve a) and electrostrictive, $\alpha_{xx} = \alpha_{xz}$ (curve b) nonlinearities. Fig. 7 shows the

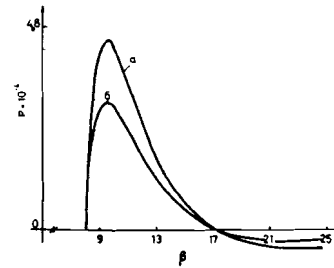


Fig. 6. Dependence of the power flow P on the effective index β for parameter value $\omega = 3.66 \times 10^{15} \text{ rad/s}$, $\epsilon_c = \epsilon_x = \epsilon_z = 2.405$, $\epsilon_s = -2.5$, $\alpha_{xx} = \alpha_{zz} = 6.4 \times 10^{-12} \text{ m}^2 \text{V}^{-2}$ and (a) $\alpha_{xx} = 3\alpha_{xz}$; (b) $\alpha_{xx} = \alpha_{xz}$.

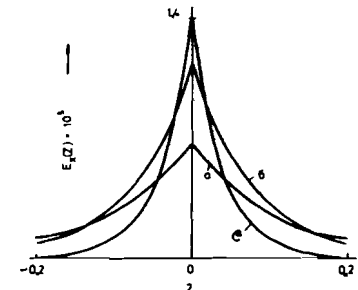


Fig. 7. E_x versus transverse coordinate z for the case (a) in Fig. 6 and (a) $\beta = 9$, (b) $\beta = 13$, (c) $\beta = 25$.

3. Transverse Electric Polarized Nonlinear Optical Waves Guided by Thin Dielectric Films

3.1. Nonlinear guided wave propagation in three layer structures with Kerr-law media

A guided wave is an electromagnetic field that is guided by media of high refractive index. A dielectric slab is the simplest example of an optical waveguide; it is actually employed for light guidance in integrated optics circuits (see, for example /87-89/). A slab waveguide is a thin dielectric film of thickness d and refractive index n_f surrounded by media of lower refractive indices: the substrate with refractive index n_s and the cladding with refractive index n_c . For thin-film waveguides and TE waves (polarized along the y axis) the only nonvanishing component of the electric field is

$$E_y^I(z) = E_s \exp(k_0 q_s z) \quad , \quad z < 0 \quad (3.1)$$

$$E_y^{II}(z) = E_f \cos(k_0 q_f z - \Phi_{sf}) \quad , \quad 0 < z < d \quad (3.2)$$

$$E_y^{III}(z) = E_c \exp[-k_0 q_c (z-d)] \quad , \quad z > d \quad (3.3)$$

where $q_s = (\beta^2 - n_s^2)^{1/2}$, $q_f = (n_f^2 - \beta^2)^{1/2}$, $q_c = (\beta^2 - n_c^2)^{1/2}$.

From the continuity of E_y and dE_y/dz at the interfaces $z = 0$ and $z = d$ we obtain the dispersion relation:

$$\operatorname{tg}(\kappa_0 q_f d) = \frac{q_f(q_s + q_c)}{(q_f^2 - q_s q_c)}. \quad (3.4)$$

Equation (3.4) can be rewritten in the form (constructive interference condition):

$$\kappa_0 q_f d = \Phi_{sf} + \Phi_{cf} + m\pi, \quad m = 0, 1, 2, \dots \quad (3.5)$$

where $\operatorname{tg} \Phi_{sf} = q_s/q_f$ and $\operatorname{tg} \Phi_{cf} = q_c/q_f$. Solutions of eq. (3.5) can exist for a discrete number of values of m and are labelled TEm ($m=0, 1, 2, \dots$). Note also that we have the following relations for the field amplitudes:

$$E_s^2(n_f^2 - n_s^2) = E_f^2(n_f^2 - \beta^2) = E_c^2(n_f^2 - n_c^2). \quad (3.6)$$

It remains to relate the amplitude coefficient E_f of the electromagnetic field to the power carried by the mode. The guided wave power flow is obtained by integrating the x component of the Poynting vector:

$$P = \frac{1}{4} \beta \left(\frac{\epsilon_0}{\mu_0} \right)^{1/2} E_f^2 d_{\text{eff}}, \quad (3.7)$$

where $d_{\text{eff}} = d + (\kappa_0 q_c)^{-1} (\kappa_0 q_s)^{-1}$ is the effective thickness of the thin film waveguide. Therefore, from eq. (3.7) we can find the field amplitude E_f as a function of the power flow P and the effective index β .

There are also transverse magnetic (TM) polarized modes with the magnetic field polarized along the Y -axis, i.e., $H_y \neq 0$ and with $E_x \neq 0$ and $E_z \neq 0$ (see /87/). Thus TM-polarized waves exhibit two electric field components, one parallel (E_x) to the wave vector and one perpendicular (E_z) to the surface (a complication for nonlinear optics). Note that the dispersion relation for TM-modes of a linear asymmetric waveguide is given by eq. (3.4), with q_f replaced by q_s/ϵ_γ , where $\gamma = s, f, c$. A guided wave version of the slowly varying phase and amplitude approximation has been developed for guided waves and is known as coupled mode theory /7-8/. This method is useful for analyzing the generation of new waves and for intensity-dependent refractive index phenomena. If the optical nonlinearities do not alter significantly the field distribution of the guided waves the coupled mode theory can be used to calculate the intensity-dependent wavevector or phase shift /9/. In the case that the optically induced refractive index change is comparable with or larger than the index differences $n_f - n_c$, $n_f - n_s$ which exist at low-powers between the dielectric film and the bounding media, both the field profiles and propagation constants are power-dependent; and coup-

led mode theory which is essentially a form of first-order perturbation theory is inadequate to obtain even qualitative results. In this case an exact theory must be used. For Kerr-law media and TE surface guided waves the nonlinear wave equation can be solved analytically.

The asymmetric dielectric layered structure we consider consists of an optically linear medium with refractive index n_s (the substrate) occupying the half-space $z < 0$ (region I), a dielectric film of thickness d with refractive index n_f in region II ($0 < z < d$) and a nonlinear Kerr-law self-focusing cladding described by the dielectric function $\epsilon = \epsilon_c + \alpha_c |\vec{E}|^2$, $\alpha_c > 0$ in the region III ($z > d$).

The Maxwell's equations for the x -independent guided wave fields are:

$$\frac{d^2 E_y^I}{dz^2} - \kappa_0^2 (\beta^2 - \epsilon_s) E_y^I = 0, \quad z < 0 \quad (3.8)$$

$$\frac{d^2 E_y^{II}}{dz^2} - \kappa_0^2 (\beta^2 - \epsilon_f) E_y^{II} = 0, \quad 0 < z < d \quad (3.9)$$

$$\frac{d^2 E_y^{III}}{dz^2} - \kappa_0^2 (\beta^2 - \epsilon_c) E_y^{III} + \alpha_c \kappa_0^2 (E_y^{III})^3 = 0, \quad z > d \quad (3.10)$$

The exact solutions of eqs. (3.8), (3.9) and (3.10) for $\alpha_c > 0$ (self-focusing optical nonlinearities) and $\beta < n_f$ can be written as:

$$E_y^I(z) = (\alpha_c)^{-1/2} \tilde{A} \exp(\kappa_0 q_s z), \quad z < 0 \quad (3.11)$$

$$E_y^{II}(z) = (\alpha_c)^{-1/2} \tilde{A} [\cos(\kappa_0 q_f z) + \frac{q_s}{q_f} \sin(\kappa_0 q_f z)], \quad 0 < z < d \quad (3.12)$$

$$E_y^{III}(z) = \left(\frac{2}{\alpha_c} \right)^{1/2} q_c \left\{ \operatorname{ch}[\kappa_0 q_c (z - z_c)] \right\}^{-1}, \quad z > d, \quad (3.13)$$

where

$$\tilde{A} = [2(1 - \tilde{\nu})]^{1/2} q_c [\cos(\kappa_0 q_f d) + \frac{q_s}{q_f} \sin(\kappa_0 q_f d)]^{-1} \quad (3.14)$$

$$\tilde{\nu} = \operatorname{th}[\kappa_0 q_c (z_c - d)]. \quad (3.15)$$

The dispersion relations are obtained from matching the tangential electric and magnetic fields at the interface /30, 90/:

$$\operatorname{tg}(\kappa_0 q_f d) = \frac{q_f(q_s - \nu q_c)}{(q_f^2 + \nu q_s q_c)}. \quad (3.16)$$

This result is very similar to the linear case with the exception that q_c is replaced by $(-vq_c)$. When $\alpha \rightarrow 0$, then $z_c \rightarrow -\infty$, $v \rightarrow -1$ and we obtain the dispersion relation of TE polarized modes of the linear asymmetric thin-film waveguide (see eq. (3.4)).

For $\beta > n_f$ the exact solution of Maxwell's equations (3.8), (3.9) and (3.10) are:

$$E_y^I(z) = \alpha_c^{-1/2} \tilde{B} \exp(\kappa_0 q_s z), \quad z < 0 \quad (3.17)$$

$$E_y^{II}(z) = \alpha_c^{-1/2} \tilde{B} \left[\frac{q_s + \tilde{q}_f}{2\tilde{q}_f} \exp(\kappa_0 \tilde{q}_f z) + \frac{\tilde{q}_f - q_s}{2\tilde{q}_f} \exp(-\kappa_0 \tilde{q}_f z) \right] \quad (3.18)$$

and $E_y^{III}(z)$ is given by eq. (3.13).

Here $\tilde{q}_f = (\beta^2 - n_f^2)^{1/2}$ and

$$\tilde{B} = [2(1-v^2)]^{1/2} q_c \left[\text{ch}(\kappa_0 \tilde{q}_f d) + \frac{q_s}{\tilde{q}_f} \text{sh}(\kappa_0 \tilde{q}_f d) \right]^{-1}. \quad (3.19)$$

The dispersion relation obtained by ensuring the continuity of E_y and dE_y/dz across the interfaces $z=0$ and $z=d$ is

$$\text{th}(\kappa_0 \tilde{q}_f d) = \frac{\tilde{q}_f (vq_c - q_s)}{(\tilde{q}_f^2 - vq_s q_c)}, \quad (3.20)$$

where v is given by eq. (3.15).

The guided wave power per unit length along the y -axis is obtained in the usual way by integrating the Poynting vector over the depth dimension z :

$$P = \frac{\beta}{2c\mu_0} \int_{-\infty}^{\infty} E_y^2(z) dz = P_s + P_f + P_c. \quad (3.21)$$

For $\beta < n_f$ we have (see /91,92/):

$$P_s = \frac{1}{2} P_0 \beta \frac{\tilde{A}^2}{q_s} \quad (3.22)$$

$$P_f = \frac{1}{2} P_0 \beta \tilde{A}^2 \left\{ \kappa_0 d \left(1 + \frac{q_s^2}{\tilde{q}_f^2} \right) + \frac{1}{\tilde{q}_f} \sin(\kappa_0 q_f d) \times \left[\left(1 - \frac{q_s^2}{\tilde{q}_f^2} \right) \cos(\kappa_0 q_f d) + 2 \frac{q_s}{\tilde{q}_f} \sin(\kappa_0 q_f d) \right] \right\} \quad (3.23)$$

$$P_c = 2P_0 \beta q_c (1+v). \quad (3.24)$$

For $\beta > n_f$ we obtain

$$P_s = \frac{1}{2} P_0 \beta \frac{\tilde{B}^2}{q_s} \quad (3.25)$$

$$P_f = \frac{1}{2} P_0 \beta \tilde{B}^2 \left\{ \kappa_0 d \left(1 - \frac{q_s^2}{\tilde{q}_f^2} \right) + \frac{1}{\tilde{q}_f} \text{sh}(\kappa_0 \tilde{q}_f d) \times \left[\left(1 + \frac{q_s^2}{\tilde{q}_f^2} \right) \text{ch}(\kappa_0 \tilde{q}_f d) + 2 \frac{q_s}{\tilde{q}_f} \text{sh}(\kappa_0 \tilde{q}_f d) \right] \right\} \quad (3.26)$$

and P_c is given by eq. (3.24).

We consider the liquid crystal MBBA ($n_c = 1.55$, $n_{2c} = 10^{-9} \text{ m}^2/\text{W}$) as the nonlinear cladding medium deposited on a glass waveguide ($n_f = 1.61$, $n_s = 1.52$). The existence of the nonlinear cladding affects the cut-off conditions for an asymmetric film waveguide. As is well known, a linear asymmetric optical waveguide ($n_c \neq n_s$) cannot support guided waves below a critical thickness d_{cr} (see, e.g. /87,88/).

In the case of an asymmetric nonlinear optical waveguide there is a power threshold for TE₀ wave propagation for film thicknesses $d < d_{cr}$ (see Fig. 8 for $d/\lambda = 0.1$). This phenomenon can be used as a

lower power threshold device, i.e., one which begins to transmit above a certain minimum power. A lower power threshold device can also be achieved with a saturable self-focusing cladding provided that the saturation value n_{sat} is not too large.

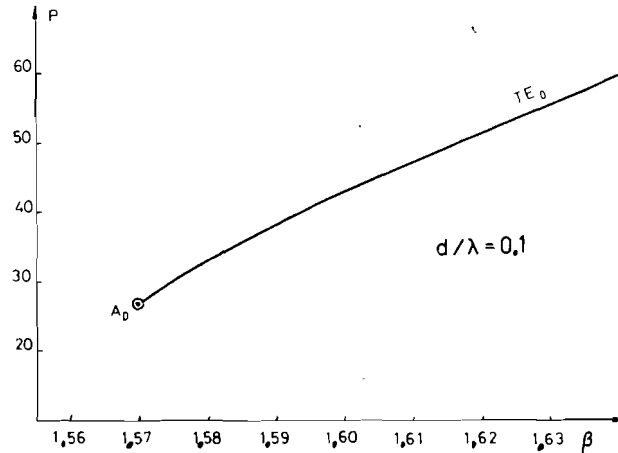


Fig. 8. TE₀ guided wave power versus effective index β . Here $n_c = 1.55$, $n_{2c} = 10^{-9} \text{ m}^2/\text{W}$, $n_s = 1.52$, $n_f = 1.61$, $\lambda = 0.515 \mu\text{m}$.

The dependence of the guided wave power on the effective index β is shown in Fig. 9 for $d = 2 \mu\text{m}$, $n_c = n_s = 1.55$, $n_{2c} = 10^{-9} \text{ m}^2/\text{W}$, $n_f = 1.57$. The unique features of the TE₀ solution are the existence of wave propagation for $\beta > n_f$ and of the local maximum in the guided wa-

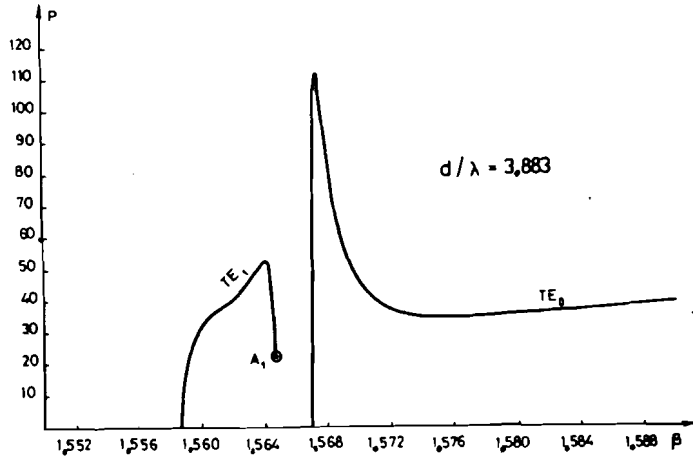


Fig. 9. Guided wave power versus effective index β . Here $n_c = n_s = 1.55$, $n_{2c} = 10^{-9} \text{ m}^2/\text{W}$, $n_f = 1.57$, $d = 2 \mu\text{m}$, $\lambda = 0.515 \mu\text{m}$ (after /93/).

The evolution of the TE_0 and TE_1 field distribution with increasing β is shown in Fig. 10. This illustrates one of the characteristic features of nonlinear guided waves, namely power dependent field distributions. As shown in Fig. 10, as β increases, the TE_0

field maximum gradually narrows and moves into the nonlinear self-focusing cladding. With increasing β the TE_1 field maximum nearest the nonlinear cladding shifts into that medium.

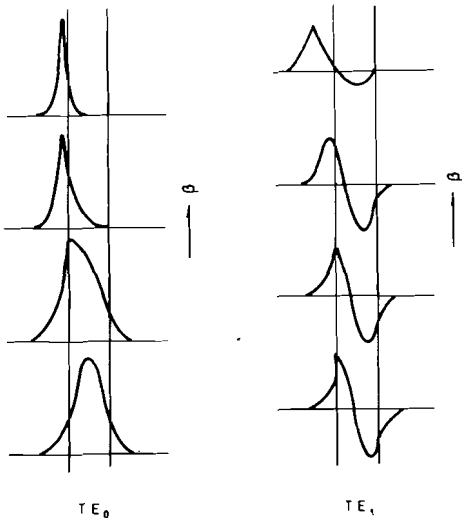


Fig. 10. Field distributions associated with TE_0 and TE_1 nonlinear guided waves. The field evolution with increasing β is shown (after /14/).

ve power. For TE_1 wave shown in Fig. 9, the value of β never exceeds n_f and there is an absolute maximum in the guided wave power. Moreover, the TE_1 branch terminates at some value of $\beta < n_f$ (see Fig. 9).

The variation in the guided wave power with propagation constant β for $d/\lambda = 6$ shown in Fig. 11 illustrates that the higher order TE_m ($m \geq 1$) branches all terminate at some values of $\beta < n_f$. For a self-focusing cladding there is an absolute maximum in the power which can be propagated in any TE_m ($m \geq 1$) guided wave. For all film thicknesses, the lowest order TE_0 branch degenerate at high powers

into a self-focused surface wave guided by the nonlinear interface between the film and the cladding media. Clearly, these nonlinear guided waves can be used for optical limiters in a variety of applications.

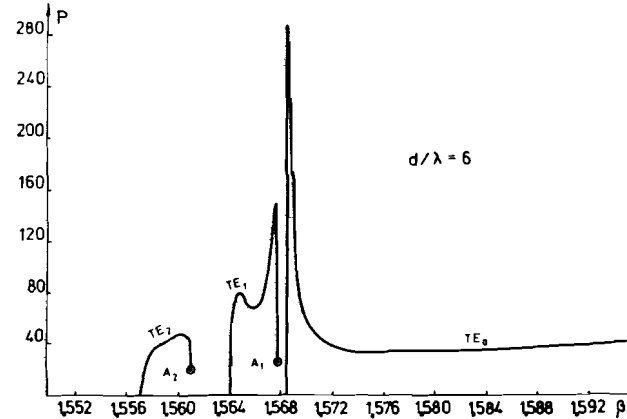


Fig. 11. Guided wave power versus effective index β . Here $n_c = n_s = 1.55$, $n_{2c} = 10^{-9} \text{ m}^2/\text{W}$, $n_f = 1.57$, $d/\lambda = 6$ and $\lambda = 0.515 \mu\text{m}$.

The limiting action for the case of a self-focusing nonlinear cladding has been demonstrated for TE_1 waves experimentally (see /56/).

In what follows we consider a symmetric thin-film waveguide which consists of a dielectric thin film of thickness d and refractive index n_f bounded on both sides by identical self-focusing Kerr-law media ($n_s = n_c$ and $d_s = d_c > 0$). The dielectric film fills the region II ($-d/2 \leq z \leq d/2$) and the two nonlinear dielectrics fill the half spaces I ($z < -d/2$) and III ($z > d/2$), respectively. The Maxwell equations for TE-polarized waves are:

$$\frac{d^2 E_y^I}{dz^2} - \kappa_0^2 (\beta^2 - \epsilon_c) E_y^I + \kappa_0^2 d_c (E_y^I)^3 = 0, \quad z < -d/2 \quad (3.27)$$

$$\frac{d^2 E_y^{II}}{dz^2} - \kappa_0^2 (\beta^2 - \epsilon_f) E_y^{II} = 0, \quad -d/2 < z < d/2 \quad (3.28)$$

$$\frac{d^2 E_y^{\text{III}}}{dz^2} - \kappa_0^2 (\beta^2 - \epsilon_c) E_y^{\text{III}} + \kappa_0^2 \alpha_c (E_y^{\text{III}})^3 = 0, \quad z > d/2. \quad (3.29)$$

The exact solutions of differential equations (3.27), (3.28) and (3.29) in the case $\alpha_c > 0$ (self-focusing optical nonlinearity) are:

$$E_y^{\text{I}}(z) = \left(\frac{2}{\alpha_c}\right)^{1/2} q_c \left\{ \text{ch} [k_0 q_c (z - z_s)] \right\}^{-1}, \quad z < -d/2 \quad (3.30)$$

$$E_y^{\text{II}}(z) = \begin{cases} A_1 \cos [k_0 q_f (z - z_f)] & , \beta < n_f \\ A_2 \text{ch} [k_0 \tilde{q}_f (z - z_f)] & , \beta > n_f \end{cases} \quad -d/2 < z < d/2 \quad (3.31)$$

$$E_y^{\text{III}}(z) = \left(\frac{2}{\alpha_c}\right)^{1/2} q_c \left\{ \text{ch} [k_0 q_c (z - z_c)] \right\}^{-1}, \quad z > d/2. \quad (3.32)$$

From the boundary conditions we are left with an equation for the unknown z_f :

$$\begin{aligned} & \left\{ 1 - b_1^2 \text{th}^2 [k_0 \tilde{q}_f (\frac{d}{2} - z_f)] \right\} \text{ch}^2 [k_0 \tilde{q}_f (\frac{d}{2} + z_f)] - \\ & - \left\{ 1 - b_1^2 \text{th}^2 [k_0 \tilde{q}_f (\frac{d}{2} + z_f)] \right\} \text{ch}^2 [k_0 \tilde{q}_f (\frac{d}{2} - z_f)] = 0, \end{aligned} \quad (3.33)$$

where $b_1 = \tilde{q}_f / q_c$.

Equation (3.33) has a unique solution $z_f = 0$ for all $\beta > n_f$. The solution (3.31) for which $z_f = 0$ corresponds to the symmetric wave (S) of the symmetric three layer planar structure. In this case the field distribution is symmetric to the center of the waveguiding thin film and $z_c = -z_s$. The eigenvalue equations for the symmetric branch are:

$$\text{th} [k_0 q_c (\frac{d}{2} + z_c)] = b_2 \text{tg} (k_0 q_f \frac{d}{2}), \quad \beta < n_f \quad (3.34)$$

$$\text{th} [k_0 q_c (\frac{d}{2} + z_c)] = -b_1 \text{th} (k_0 \tilde{q}_f \frac{d}{2}), \quad \beta > n_f, \quad (3.35)$$

where $b_2 = q_f / q_c$.

Note that if $\alpha_c > 0$, then $z_c \rightarrow +\infty$ and eq. (3.34) reduces to the well-known dispersion relation for the symmetric (even) modes of the symmetric dielectric waveguide:

$$\text{tg} (k_0 q_f \frac{d}{2}) = \frac{q_c}{q_f}. \quad (3.36)$$

For the symmetric solution (S) the amplitudes of the electric field inside the dielectric thin film are given by:

$$A_1^2 = \frac{2}{\alpha_c} q_c^2 \left[\cos (k_0 q_f \frac{d}{2}) \right]^{-2} \left[1 - b_2^2 \text{tg}^2 (k_0 q_f \frac{d}{2}) \right], \quad \beta < n_f \quad (3.37)$$

$$A_2^2 = \frac{2}{\alpha_c} q_c^2 \left[\text{ch} (k_0 \tilde{q}_f \frac{d}{2}) \right]^{-2} \left[1 - b_1^2 \text{th}^2 (k_0 \tilde{q}_f \frac{d}{2}) \right], \quad \beta > n_f \quad (3.38)$$

Next we obtain the dispersion relations for the antisymmetric wave (AS) of the symmetric thin-film waveguide. For this purpose we write down the second solution of Maxwell equation (3.28) inside the film layer:

$$E_y^{\text{IV}}(z) = \begin{cases} B_1 \sin [k_0 q_f (z - z_f)] & , \beta < n_f \\ B_2 \text{sh} [k_0 \tilde{q}_f (z - z_f)] & , \beta > n_f. \end{cases} \quad (3.39)$$

In this case the equations for the unknown z_f have the form:

$$\left\{ 1 - b_2^2 \text{ctg}^2 [k_0 q_f (\frac{d}{2} - z_f)] \right\} \sin^2 [k_0 q_f (\frac{d}{2} + z_f)] - \quad (3.40)$$

$$- \left\{ 1 - b_2^2 \text{ctg}^2 [k_0 q_f (\frac{d}{2} + z_f)] \right\} \sin^2 [k_0 q_f (\frac{d}{2} - z_f)] = 0$$

for $\beta < n_f$ and

$$\left\{ 1 - b_1^2 \text{th}^2 [k_0 \tilde{q}_f (\frac{d}{2} - z_f)] \right\} \text{sh}^2 [k_0 \tilde{q}_f (\frac{d}{2} + z_f)] -$$

$$- \left\{ 1 - b_1^2 \text{th}^2 [k_0 \tilde{q}_f (\frac{d}{2} + z_f)] \right\} \text{sh}^2 [k_0 \tilde{q}_f (\frac{d}{2} - z_f)] = 0. \quad (3.41)$$

for $\beta > n_f$.

It is easily verified that eqs. (3.40) and (3.41) have the solution $z_f = 0$. This solution corresponds to the antisymmetric wave (AS) of the symmetric layered structure. We notice that eqs. (3.40) and (3.41) have also solutions $z_f \neq 0$, i.e., the asymmetric wave (A) propagating in a nonlinear symmetric layered structure. The asymmetric wave only exists above a definite power threshold [23]. From the boundary conditions we get the following dispersion relations for the antisymmetric wave (AS):

$$\text{th} [k_0 q_c (\frac{d}{2} + z_c)] = -b_2 \text{ctg} (k_0 q_f \frac{d}{2}), \quad \beta < n_f \quad (3.42)$$

$$\text{th} [k_0 q_c (\frac{d}{2} + z_c)] = -b_1 \text{cth} (k_0 \tilde{q}_f \frac{d}{2}), \quad \beta > n_f. \quad (3.43)$$

If $\alpha_c > 0$, then $z_c \rightarrow +\infty$ and from eq. (3.42) we obtain the dispersion relation for the antisymmetric (odd) modes of the linear symmetric waveguide:

$$\text{ctg} (k_0 q_f \frac{d}{2}) = -\frac{q_c}{q_f}. \quad (3.44)$$

The amplitudes B_1 and B_2 of the electric field inside the linear medium in the case of the antisymmetric solution are given by

$$B_1^2 = \frac{2}{\alpha_c} q_c^2 [\sin(\kappa_0 q_f \frac{d}{2})]^{-2} [1 - b_2^2 \text{ctg}^2(\kappa_0 q_f \frac{d}{2})], \beta < n_f \quad (3.45)$$

$$B_2^2 = \frac{2}{\alpha_c} q_c^2 [\text{sh}(\kappa_0 \tilde{q}_f \frac{d}{2})]^{-2} [1 - b_2^2 \text{th}^2(\kappa_0 \tilde{q}_f \frac{d}{2})], \beta > n_f. \quad (3.46)$$

In the case of the symmetric wave (S) the time averaged total guided wave power in watts per meter of wavefront is expressed as

$$P = 4P_0 \beta q_c (1-r_2) \left\{ 1 + \frac{q_c}{4} (1+r_2) [\cos(\kappa_0 q_f \frac{d}{2})]^{-2} \left[\kappa_0 d + \frac{\sin(\kappa_0 q_f d)}{q_f} \right] \right\} \quad (3.47)$$

for $\beta < n_f$ and

$$P = 4P_0 \beta q_c (1-r_2) \left\{ 1 + \frac{q_c}{4} (1+r_2) [\text{ch}(\kappa_0 \tilde{q}_f \frac{d}{2})]^{-2} \left[\kappa_0 d + \frac{\text{sh}(\kappa_0 \tilde{q}_f d)}{\tilde{q}_f} \right] \right\} \quad (3.48)$$

for $\beta > n_f$, where

$$r_1 = -b_1 \text{th}(\kappa_0 \tilde{q}_f \frac{d}{2}), \quad r_2 = b_2 \text{tg}(\kappa_0 q_f \frac{d}{2}). \quad (3.49)$$

Equations (3.47) and (3.48) give us the dependence $\omega = \omega(\beta, P)$, i.e., the dispersion relation for the nonlinear symmetric wave (S). We remark that for $P=0$, eq. (3.47) gives $1-r_2 = 0$, i.e., the dispersion relation of TE-polarized symmetric (even) modes of the symmetric linear waveguide. It is also easy to verify that as $d \rightarrow \infty$, eq. (3.48) yields double the energy flux of the surface waves at a nonlinear interface (see Section 2).

In a similar manner, making use of eqs. (3.45) and (3.46) we obtain the power flow in the nonlinear antisymmetric solution (AS):

$$P = 4P_0 \beta q_c (1-t_2) \left\{ 1 + \frac{q_c}{4} (1+t_2) [\sin(\kappa_0 q_f \frac{d}{2})]^{-2} \left[-\frac{\sin(\kappa_0 q_f d)}{q_f} + \kappa_0 d \right] \right\} \quad (3.50)$$

for $\beta < n_f$ and

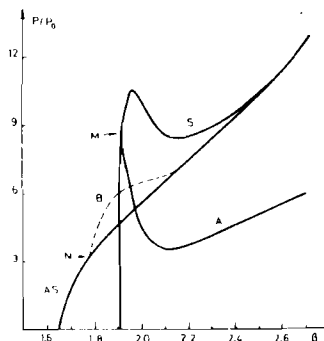
$$P = 4P_0 \beta q_c (1-t_1) \left\{ 1 + \frac{q_c}{4} (1+t_1) [\text{sh}(\kappa_0 \tilde{q}_f \frac{d}{2})]^{-2} \left[\frac{\text{sh}(\kappa_0 \tilde{q}_f d)}{\tilde{q}_f} - \kappa_0 d \right] \right\} \quad (3.51)$$

for $\beta > n_f$, where

$$t_1 = -b_1 \text{th}(\kappa_0 \tilde{q}_f \frac{d}{2}), \quad t_2 = -b_2 \text{ctg}(\kappa_0 q_f \frac{d}{2}). \quad (3.52)$$

Here, too, it is easily seen that at $P=0$, eq. (3.50) reduces to $1-t_2 = 0$, i.e., the dispersion relation for antisymmetric (odd) modes of the symmetric linear waveguide, while as $d \rightarrow \infty$, eq. (3.51) gives double the power flow of the nonlinear surface waves.

For a material system with complete symmetry, i.e., $n_c = n_s$ and $n_{2c} = n_{2s} > 0$ (self-focusing nonlinearities) one expects that at high powers self-focused fields can occur in one or both boundary media. The dependence of the dimensionless flux P/P_0 on the propagation constant β is shown in Fig. 12 for a symmetric layered structure with the parameters: $n_f = 2.0$, $n_c = n_s = 1.5$, $d/\lambda = 0.6$ (see /23/).



Branch S exhibit field distributions symmetric with respect to the film center (symmetric TEO branch).

Fig. 12.

Normalized power flow P/P_0 versus effective index β for a symmetric layered structure. Here $n_f = 2.0$, $n_c = n_s = 1.5$, $d/\lambda = 0.6$. The curves are marked as follows: S - for symmetric TEO branch, A - for asymmetric TEO branch, AS - for symmetric TE_1 branch, B - for asymmetric TE_1 branch (after /23/).

In this case with increasing power flow a field minimum develops in the center of the film and two symmetric field maxima move into the cladding and substrate media. Branch A only exists above a power threshold and the associated fields are self-focused in either the cladding or the substrate (asymmetric TEO branch). For curve AS the field distributions retain symmetry with respect to the center of the thin film (symmetric TE_1 branch). This branch evolves from the usual low power TE_1 mode with field extrema in the film, to a high power TE_1 branch with symmetric field maxima localized in the two nonlinear bounding media. Curve B has a power threshold and is similar to that labelled A since the field distributions are asymmetric with respect to the film center (asymmetric TE_1 branch).

In what follows we will derive the exact dispersion relations for TE polarized guided waves in a planar structure consisting of an optically linear dielectric film embedded in dissimilar optically nonlinear unbounded media. The three layer waveguiding structure consists of a nonlinear substrate characterized by the Kerr dielectric

function $\varepsilon = \varepsilon_s + \alpha_s |\vec{E}|^2$ in the region I ($z < 0$), a thin dielectric film of thickness d with dielectric constant ε_f in region II ($0 < z < d$) and a nonlinear cladding characterized by the Kerr dielectric function $\varepsilon = \varepsilon_c + \alpha_c |\vec{E}|^2$ in the region III ($z > d$). The Maxwell equations for TE polarized waves propagating along the x axis with effective index β are

$$\frac{d^2 E_Y^I}{dz^2} - \kappa_0^2 (\beta^2 - \varepsilon_s) E_Y^I + \kappa_0^2 \alpha_s (E_Y^I)^3 = 0, \quad z < 0 \quad (3.53)$$

$$\frac{d^2 E_Y^{II}}{dz^2} - \kappa_0^2 (\beta^2 - \varepsilon_f) E_Y^{II} = 0 \quad 0 < z < d \quad (3.54)$$

$$\frac{d^2 E_Y^{III}}{dz^2} - \kappa_0^2 (\beta^2 - \varepsilon_c) E_Y^{III} + \kappa_0^2 \alpha_c (E_Y^{III})^3 = 0, \quad z > d. \quad (3.55)$$

For the nonlinear substrate medium the field solutions are

$$E_Y^I(z) = \left(\frac{2}{\alpha_s}\right)^{1/2} q_s \left\{ \text{ch} [k_0 q_s (z_s - z)] \right\}^{-1}, \quad z < 0 \quad (3.56)$$

for $\alpha_s > 0$ (self-focusing nonlinearity) and

$$E_Y^I(z) = \left(\frac{2}{|\alpha_s|}\right)^{1/2} q_s \left\{ \text{sh} [k_0 q_s (z_s - z)] \right\}^{-1}, \quad z < 0 \quad (3.57)$$

for $\alpha_s < 0$ (self-defocusing nonlinearity), where $q_s = (\beta^2 - \varepsilon_s)^{1/2}$.

The fields inside the optically linear dielectric film are written as

$$E_Y^{II}(z) = E_Y^{II}(0) \left\{ \cos(k_0 q_f z) + \frac{q_s}{q_f} [\text{th}(k_0 q_s z_s)]^{\pm 1} \sin(k_0 q_f z) \right\}, \quad (3.58)$$

where $0 < z < d$, $q_f = (\varepsilon_f - \beta^2)^{1/2}$ and the ± 1 signs refer to the cases $\alpha_s > 0$ and $\alpha_s < 0$, respectively.

For the nonlinear cladding medium the nonlinear wave solutions are

$$E_Y^{III}(z) = \left(\frac{2}{\alpha_c}\right)^{1/2} q_c \left\{ \text{ch} [k_0 q_c (z_c - z)] \right\}^{-1}, \quad z > d \quad (3.59)$$

for $\alpha_c > 0$ and

$$E_Y^{III}(z) = \left(\frac{2}{|\alpha_c|}\right)^{1/2} q_c \left\{ \text{sh} [k_0 q_c (z_c - z)] \right\}^{-1}, \quad z > d \quad (3.60)$$

for $\alpha_c < 0$, where $q_c = (\beta^2 - \varepsilon_c)^{1/2}$.

The dispersion relations are obtained from matching the tangential electric and magnetic fields at the film-cladding interface ($z = d$):

$$\text{tg}(\kappa_0 q_f d) = \frac{q_f (v_s^{\pm 1} q_s + v_c^{\pm 1} q_c)}{(q_f^2 - v_s^{\pm 1} v_c^{\pm 1} q_s q_c)}, \quad (3.61)$$

where $v_s = \text{th}(\kappa_0 q_s z_s)$, $v_c = \text{th}[\kappa_0 q_c (d - z_c)]$ and ± 1 signs refer to self-focusing and self-defocusing nonlinearities, respectively. This result is very similar to the linear case with the exception that q_s and q_c are replaced by $v_s^{\pm 1} q_s$ and $v_c^{\pm 1} q_c$, respectively. When $\alpha_s \rightarrow 0$, $\alpha_c \rightarrow 0$, then $z_s \rightarrow +\infty$, $z_c \rightarrow -\infty$, $v_s \rightarrow +1$, $v_c \rightarrow +1$ and from eq. (3.61) we get the dispersion relation for TE polarized modes of the linear asymmetric waveguide (see eq. (3.4)).

For $\beta > n_f$ the analytical solution of Maxwell equation (3.54) is

$$E_Y^{II}(z) = E_Y^{II}(0) \left\{ \text{ch}(\kappa_0 \tilde{q}_f z) + \frac{q_s}{\tilde{q}_f} [\text{th}(\kappa_0 q_s z_s)]^{\pm 1} \sin(\kappa_0 \tilde{q}_f z) \right\}, \quad (3.62)$$

where $0 < z < d$, $\tilde{q}_f = (\beta^2 - \varepsilon_f)^{1/2}$ and the ± 1 signs refer to the cases $\alpha_c > 0$ and $\alpha_c < 0$, respectively.

Continuity of the magnetic fields gives the dispersion relation for $\beta > n_f$:

$$\text{th}(\kappa_0 \tilde{q}_f d) = - \frac{\tilde{q}_f (v_s^{\pm 1} q_s + v_c^{\pm 1} q_c)}{(\tilde{q}_f^2 + v_s^{\pm 1} v_c^{\pm 1} q_s q_c)}. \quad (3.63)$$

The guided wave power per unit length along the y -axis is $P = P_s + P_f + P_c$, where

$$P_s = \frac{\beta q_s}{\kappa_0 n_s^2 n_{2s}} (1 - v_s^{\pm 1}) \quad (3.64)$$

$$P_c = \frac{\beta q_c}{\kappa_0 n_c^2 n_{2c}} (1 - v_c^{\pm 1}) \quad (3.65)$$

$$P_f = \frac{\beta q_s^2}{2 \kappa_0 n_s^2 n_{2s}} (1 - v_s^{\pm 2}) \left\{ \kappa_0 d \left(1 + \frac{q_s^2 v_s^{\pm 2}}{q_f^2} \right) + \frac{\sin(\kappa_0 q_f d)}{q_f} \left[\left(1 - \frac{q_s^2 v_s^{\pm 2}}{q_f^2} \right) \cos(\kappa_0 \tilde{q}_f d) + 2 \frac{q_s v_s^{\pm 1}}{q_f} \sin(\kappa_0 \tilde{q}_f d) \right] \right\} \quad (3.66)$$

for $\beta < n_f$ and

$$P_f = \frac{\beta q_s^2}{2 \kappa_0 n_s^2 n_{2s}} (1 - v_s^{\pm 2}) \left\{ \kappa_0 d \left(1 - \frac{q_s^2 v_s^{\pm 2}}{q_f^2} \right) + \frac{\text{sh}(\kappa_0 \tilde{q}_f d)}{q_f} \left[\left(1 + \frac{q_s^2 v_s^{\pm 2}}{q_f^2} \right) \text{ch}(\kappa_0 \tilde{q}_f d) + 2 \frac{q_s v_s^{\pm 1}}{q_f} \text{sh}(\kappa_0 \tilde{q}_f d) \right] \right\} \quad (3.67)$$

for $\beta > n_f$ (see [93]).

Since the constants of integrations Z_S and Z_C in eqs. (3.56), (3.57), (3.59) and (3.60) are related via the boundary conditions and are dependent on the power carried by the nonlinear guided wave, then the propagation constant β obtained by solving the dispersion relations (3.61) and (3.63) becomes power dependent.

Next we show that a knowledge of the field shapes is not necessary, however, in order to determine the dispersion relations of the problem /29,94,95/. The Maxwell equations (3.53), (3.54) and (3.55) integrate to

$$\left(\frac{dE_y^I}{dz}\right)^2 - \kappa_0^2(\beta^2 - \epsilon_s)(E_y^I)^2 + \frac{\kappa_0^2 \alpha_s}{2}(E_y^I)^4 = 0 \quad (3.68)$$

$$\left(\frac{dE_y^{II}}{dz}\right)^2 - \kappa_0^2(\beta^2 - \epsilon_f)(E_y^{II})^2 = C_f \quad (3.69)$$

$$\left(\frac{dE_y^{III}}{dz}\right)^2 - \kappa_0^2(\beta^2 - \epsilon_c)(E_y^{III})^2 + \frac{\kappa_0^2 \alpha_c}{2}(E_y^{III})^4 = 0 \quad (3.70)$$

because $E_y(z)$ and dE_y/dz are required to vanish as $z \rightarrow \pm\infty$; here C_f is an integration constant. Suppose that the electric fields at the boundaries $z=0$ and $z=d$ of the waveguiding film are E_0 and E_d , respectively. It is also useful, at this stage to define the quantities $\gamma_s = (\beta^2 - \epsilon_s - \frac{1}{2}\alpha_s E_0^2)^{1/2}$ and $\gamma_c = (\beta^2 - \epsilon_c - \frac{1}{2}\alpha_c E_d^2)^{1/2}$, so that the gradient of the field at $z=0$ and $z=d$ can be written as

$$\lim_{z \rightarrow 0} \frac{dE_y^I}{dz} = \pm \kappa_0 \gamma_s E_0, \quad \lim_{z \rightarrow d} \frac{dE_y^{III}}{dz} = \pm \kappa_0 \gamma_c E_d \quad (3.71)$$

Then by using eq. (3.71), the integration constant C_f can be expressed as

$$C_f = \kappa_0^2(q_f^2 + \gamma_s^2)E_0^2 = \kappa_0^2(q_f^2 + \gamma_c^2)E_d^2 \quad (3.72)$$

After some manipulation, it can be shown that the electric fields E_0^2 and E_d^2 at the boundaries of the waveguiding layer are related to each other through the following equation for a conic section (a hyperbola or an ellipse):

$$\frac{\alpha_s \alpha_c}{(\alpha_c \eta_s^2 - \alpha_s \eta_c^2)} \left(E_0^2 - \frac{\eta_s}{\alpha_s}\right)^2 - \frac{\alpha_s \alpha_c}{(\alpha_c \eta_s^2 - \alpha_s \eta_c^2)} \left(E_d^2 - \frac{\eta_c}{\alpha_c}\right)^2 = 1 \quad (3.73)$$

where $\eta_s = \epsilon_f - \epsilon_s$, $\eta_c = \epsilon_f - \epsilon_c$.

Depending on the specific material parameters of the three layer planar structure, for a particular value of E_0^2 , there may exist two, one or no values of E_d^2 . It may be noted that for a purely symmetric waveguide, i.e., $\epsilon_c = \epsilon_s$, $\alpha_c = \alpha_s$, the conic section reduces to straight lines which are perpendicular to each other:

$$(E_0^2 - E_d^2) \left[(\epsilon_f - \epsilon_s) - \frac{\alpha_s}{2} (E_0^2 + E_d^2) \right] = 0 \quad (3.74)$$

This implies that there exist both symmetric ($E_0 = E_d$) and anti-symmetric ($E_0 = -E_d$) waves in the symmetric layered structure. The third option is the asymmetric wave for which $E_0^2 \neq E_d^2$:

$$E_d^2 = \frac{2(\epsilon_f - \epsilon_s)}{\alpha_s} - E_0^2 \quad (3.75)$$

This asymmetric wave cannot exist in the linear limit (see /23,29/). The four eigenvalue equations for nonlinear guided waves ($\beta < n_f$) in the asymmetric layered structure are:

$$\cos(\kappa_0 q_f d) = \frac{(q_f^2 \pm \gamma_s \gamma_c)}{[(q_f^2 + \gamma_s^2)(q_f^2 + \gamma_c^2)]^{1/2}} \quad (3.76)$$

for even parity solution for which E_0 and E_d have the same sign ($E_0 > 0$, $E_d > 0$, or $E_0 < 0$, $E_d < 0$) and

$$\cos(\kappa_0 q_f d) = - \frac{(q_f^2 \pm \gamma_s \gamma_c)}{[(q_f^2 + \gamma_s^2)(q_f^2 + \gamma_c^2)]^{1/2}} \quad (3.77)$$

for odd parity solutions for which E_0 and E_d have opposite signs ($E_0 > 0$, $E_d < 0$ or $E_0 < 0$, $E_d > 0$), where $q_f = (z_f - \beta^2)^{1/2}$.

For nonlinear surface waves ($\beta > n_f$) the eigenvalue equations are determined from eqs. (3.76) and (3.77), i.e.,

$$\text{ch}(\kappa_0 \tilde{q}_f d) = \frac{(-\tilde{q}_f^2 \pm \gamma_s \gamma_c)}{[(\gamma_s^2 - \tilde{q}_f^2)(\gamma_c^2 - \tilde{q}_f^2)]^{1/2}} \quad (3.78)$$

for even parity waves and

$$\text{ch}(\kappa_0 \tilde{q}_f d) = - \frac{(\tilde{q}_f^2 \pm \gamma_s \gamma_c)}{[(\gamma_s^2 - \tilde{q}_f^2)(\gamma_c^2 - \tilde{q}_f^2)]^{1/2}} \quad (3.79)$$

for odd parity waves.

Next we follow the elegant analysis of Boardman and Egan /29/ to calculate the guided wave power flow without knowing the optical fields in the outside nonlinear media. The starting point of the analysis is again the first integrals (3.68), (3.69) and (3.70) of Maxwell equations.

After differentiation with respect to Z eqs. (3.68) and (3.70) become:

$$\frac{d}{dZ} \left(\frac{1}{E_Y^I} \frac{dE_Y^I}{dZ} \right) = - \frac{\kappa_0^2 \alpha_S}{2} (E_Y^I)^2 \quad (3.80)$$

$$\frac{d}{dZ} \left(\frac{1}{E_Y^{III}} \frac{dE_Y^{III}}{dZ} \right) = - \frac{\kappa_0^2 \alpha_C}{2} (E_Y^{III})^2. \quad (3.81)$$

Taking into account eqs. (3.80) and (3.81) and using

$$\lim_{Z \rightarrow -\infty} \frac{1}{E_Y^I} \frac{dE_Y^I}{dZ} = \kappa_0 q_S \quad (3.82)$$

$$\lim_{Z \rightarrow +\infty} \frac{1}{E_Y^{III}} \frac{dE_Y^{III}}{dZ} = -\kappa_0 q_C \quad (3.83)$$

after some manipulation we can calculate the power flows P_S and P_C in the nonlinear bounding media:

$$P_S = 2 \left(\frac{\epsilon_0}{\mu_0} \right)^{1/2} (2\alpha_S \kappa_0)^{-1} \beta (q_S \pm \gamma_S) \quad (3.84)$$

$$P_C = 2 \left(\frac{\epsilon_0}{\mu_0} \right)^{1/2} (2\alpha_C \kappa_0)^{-1} \beta (q_C \pm \gamma_C). \quad (3.85)$$

In the linear waveguiding film we have

$$\left[E_Y^{II}(z) \right]^2 = \frac{1}{2\kappa_0^2 q_f^2} \left[c_f - \frac{d}{dZ} \left(E_Y^{II} \frac{dE_Y^{II}}{dZ} \right) \right] \quad (3.86)$$

so that by integrating with respect to the depth variable z we obtain the following contribution to the total power flow:

$$P_f = \frac{c\epsilon_0\beta}{2} \int_0^d \left[E_Y^{II}(z) \right]^2 dz = \frac{c\epsilon_0\beta}{2} \frac{1}{2\kappa_0^2 q_f^2} \left[c_f d - \left(E_Y^{II} \frac{dE_Y^{II}}{dZ} \right)_d + \left(E_Y^{II} \frac{dE_Y^{II}}{dZ} \right)_0 \right]. \quad (3.87)$$

Further, by using eq. (3.71), the power flow in the linear film can be expressed as

$$P_f = \frac{c\epsilon_0\beta}{2} \frac{1}{2\kappa_0^2 q_f^2} \left[\kappa_0^2 (q_f^2 + \gamma_S^2) E_0^2 d \mp \kappa_0 \gamma_C E_d^2 \pm \kappa_0 \gamma_S E_0^2 \right]. \quad (3.88)$$

The total power flow in the planar structure is $P = P_S + P_f + P_C$, where P_S and P_C are given by eqs. (3.84) and (3.85), respectively, and P_f is given by eq. (3.88). Since E_d^2 is expressible in terms of E_0^2 and, through the eigenvalue equation, E_0^2 is a function of the effective index β , then the power flow P can be varied with β for a particular value of the frequency ω .

As a specific example consider the case $n_{2S} > 0$ and $n_{2C} > 0$, i.e., both bounding media exhibit self-focusing nonlinearities. This case contains by far the richest set of new phenomena /93/. We see from Fig. 13 that when $n_C = n_S$ but $n_{2C} \neq n_{2S}$, i.e., the optical non-

linearities are dissimilar, the nonlinear wave solutions evolve into two unconnected branches A and B. If, furthermore $n_C \neq n_S$, the curves shift and distort with respect to the power axis but no new features emerge.

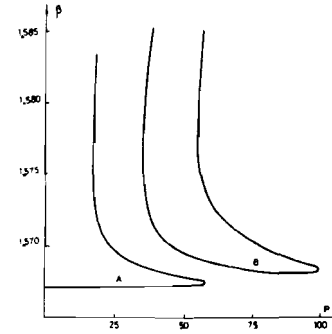


Fig. 13.

TE₀ guided wave power versus effective index β for $d = 2 \mu\text{m}$, $n_C = n_S = 1.55$, $n_f = 1.57$, $n_{2C} = 2 \times 10^{-9} \text{ m}^2/\text{W}$, $n_{2S} = 10^{-9} \text{ m}^2/\text{W}$ (after /93/)

The branch B in Fig. 13 exists only above a certain power level. The branch A which evolves from the linear case, exhibits field localization in the more nonlinear medium of the two (the cladding), i.e., degenerates at high powers into the corresponding single interface surface wave. The second branch in Fig. 13 (branch B) starts with a field extremum in the medium with the smallest nonlinearity (the substrate) and terminates with field maxima in both nonlinear bounding media. Nonlinear guided waves in the lower branch A are excited until the maximum is reached. A further increase in guided wave power can only be achieved by switching to the upper branch B on which the field distribution and hence the attenuation are different from those corresponding to lower branch A. Therefore, switching between the two branches should be accompanied by a change in the transmitted intensity. A subsequent decrease in guided wave power on upper branch B leads to switching back to the lower branch A at a much lower power than for the switch-up. Therefore, a hysteresis loop or bistability could occur /94/.

In the case of a Kerr-law waveguiding film the field solutions of Maxwell's equations are expressed in terms of Jacobian elliptic functions /16,24,95-98/.

In what follows we consider an asymmetric planar layered structure consisting of an optically linear medium (the substrate) with dielectric constant ϵ_S in region I ($z < 0$), a Kerr-law dielectric film of thickness d described by the dielectric function $\epsilon = \epsilon_f + \alpha_f |\vec{E}|^2$ in region II ($0 < z < d$) and a linear medium (the cladding) with dielectric constant ϵ_C in region III ($z > d$). The Maxwell's equa-

tions for TE-polarized waves propagating along x-axis with propagation constant β are:

$$\frac{d^2 E_Y^I}{dz^2} - \kappa_0^2 (\beta^2 - \epsilon_s) E_Y^I = 0, \quad z < 0 \quad (3.89)$$

$$\frac{d^2 E_Y^II}{dz^2} - \kappa_0^2 (\beta^2 - \epsilon_f) E_Y^II + \kappa_0^2 \alpha_f (E_Y^II)^3 = 0, \quad 0 < z < d \quad (3.90)$$

$$\frac{d^2 E_Y^III}{dz^2} - \kappa_0^2 (\beta^2 - \epsilon_c) E_Y^III = 0, \quad z > d. \quad (3.91)$$

We look for solutions localized near the surfaces of thin film with fields that fall to zero as $|z| \rightarrow \infty$. From eqs. (3.89) and (3.91) we then find:

$$E_Y^I(z) = E_0 \exp(\kappa_0 q_s z), \quad z < 0 \quad (3.92)$$

$$E_Y^III(z) = E_d \exp[-\kappa_0 q_c (z-d)], \quad z > d. \quad (3.93)$$

where $q_s = (\beta^2 - \epsilon_s)^{1/2}$ and $q_c = (\beta^2 - \epsilon_c)^{1/2}$.

Consider first the case of a self-defocusing Kerr-like nonlinearity ($\alpha_f = -|\alpha_f| < 0$). In this case we have $\beta < \eta_f$, where $\eta_f = \epsilon_f^{1/2}$ and the exact solution of eq. (3.90) can be expressed in terms of Jacobi elliptic function /99/;

$$E_Y^II(z) = \left(\frac{2}{|\alpha_f|}\right)^{1/2} m^{1/2} t \operatorname{sn}(\kappa_0 t z + \Theta/m) \quad (3.94)$$

for $0 < z < d$, where $t = (1+m)^{1/2} \tilde{q}_f$, $q_f = (\eta_f^2 - \beta^2)^{1/2}$ and Θ is a constant of integration. Here sn is a specific Jacobian elliptic function which is a sort of sine function and m is the modulus of this Jacobian function ($0 < m < 1$).

From the boundary conditions we are left with the eigenvalue equations:

$$\frac{\operatorname{cn}(\kappa_0 t d + \Theta/m) \operatorname{dn}(\kappa_0 t d + \Theta/m)}{\operatorname{sn}(\kappa_0 t d + \Theta/m)} = -\frac{q_c}{t} \quad (3.95)$$

$$\frac{\operatorname{cn}(\Theta/m) \operatorname{dn}(\Theta/m)}{\operatorname{sn}(\Theta/m)} = \frac{q_s}{t} \quad (3.96)$$

where $\operatorname{cn}^2(\Theta/m) = 1 - \operatorname{sn}^2(\Theta/m)$ and $\operatorname{dn}^2(\Theta/m) = 1 - m \operatorname{sn}^2(\Theta/m)$. Here cn is another specific Jacobian elliptic function which is a sort of cosine function.

It may be mentioned that for $m = 0$, from eq. (3.95) and (3.96) one gets the dispersion relation of TE-polarized modes of the linear asymmetric waveguide. Making use of eqs. (3.92), (3.93) and (3.94) we find the total power flow $P = P_s + P_f + P_c$ carried by the nonlinear guided wave /96-98/

$$P_s = P_0 \beta m t^2 \frac{\operatorname{sn}^2(\Theta/m)}{q_s} \quad (3.97)$$

$$P_f = 2 P_0 \beta t [\kappa_0 t d - E(\kappa_0 t d + \Theta/m) + E(\Theta/m)] \quad (3.98)$$

$$P_c = P_0 \beta m t^2 \frac{\operatorname{sn}^2(\kappa_0 t d + \Theta/m)}{q_c} \quad (3.99)$$

where $P_0 = (2 |\alpha_f| \kappa_0)^{-1} (\epsilon_0 / \mu_0)^{1/2} \frac{q_c}{q_s}$ and $E(\Theta/m)$ is the elliptic integral of the second kind.

In the approach of Akhmediev, Boltar and Eleonskii /96,97/ the propagation constant β is treated as an implicit function of the modulus of the Jacobian elliptic function. Thus solving the dispersion equations (3.95) and (3.96) one gets the values of the effective index β for every $0 < m < 1$. By means of eqs. (3.97), (3.98) and (3.99) we then find the corresponding values of the power flows P_s , P_f and P_c and therefore the dependence $P = P(\beta)$. Another, very useful technique developed by Boardman and Egan /95/ make use of the boundary field amplitudes E_0 and E_d to calculate the dependence of the propagation constant on the power flow down the guide.

In the case of a self-focusing dielectric film ($\alpha_f > 0$) the exact solution of nonlinear wave equation (3.90) is expressed as:

$$E_Y^II(z) = \left(\frac{2}{\alpha_f}\right)^{1/2} m^{1/2} t \operatorname{cn}(\kappa_0 t z + \Theta/m) \quad (3.100)$$

for $0 < z < d$, where $t = (1-2m)^{-1/2} \tilde{q}_f$ for $\beta < \eta_f$, $t = (2m-1)^{-1/2} \tilde{q}_f$ for $\beta > \eta_f$ and $\tilde{q}_f = (\beta^2 - \eta_f^2)^{1/2}$.

The dispersion relations for these nonlinear guided wave are:

$$\frac{\operatorname{sn}(\kappa_0 t d + \Theta/m) \operatorname{dn}(\kappa_0 t d + \Theta/m)}{\operatorname{cn}(\kappa_0 t d + \Theta/m)} = \frac{q_c}{t} \quad (3.101)$$

$$\frac{\operatorname{sn}(\Theta/m) \operatorname{dn}(\Theta/m)}{\operatorname{cn}(\Theta/m)} = -\frac{q_s}{t} \quad (3.102)$$

from which one gets the dependence $\beta = \beta(m)$, where m is the modulus of the Jacobian elliptic functions. By means of eqs. (3.92), (3.93) and (3.100) we obtain the following expressions for the power flows P_s , P_f and P_c in the linear substrate, nonlinear waveguiding film and linear cladding, respectively:

$$P_s = P_0 \beta m t^2 \frac{\operatorname{cn}^2(\Theta/m)}{q_s} \quad (3.103)$$

$$P_f = 2 P_0 \beta t [E(\kappa_0 t d + \Theta/m) - E(\Theta/m) - (1-m) \kappa_0 t d] \quad (3.104)$$

$$P_c = P_0 \beta m t^2 \frac{cn^2(k_0 t d + \theta/m)}{q_c}. \quad (3.105)$$

In order to find the magnitude of the power flow P for each propagation constant β , we compute numerically, using eqs. (3.101) and (3.102), the dependence of β on the modulus m of the Jacobian elliptic functions. For the material parameters used in /95/, i.e., $n_c < n_f < n_s$, all the branches TE_m ($m \geq 0$) are induced by the self-focusing nonlinearity so that nothing is propagating until a certain power threshold is reached (see Fig. 14). This threshold behaviour was first shown numerically in /96,97/ for higher order TE_m ($m \geq 1$) branches.

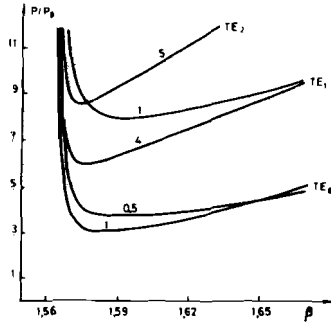


Fig. 14. Nonlinear power flow P/P_0 for TE_0, TE_1 and TE_2 waves guided by a self-focusing dielectric film versus effective index β . The curves are labelled by $k_0 d$. Here $\epsilon_s = 2.45$, $\epsilon_f = 2.3$ and $\epsilon_c = 1$ (after /95/).

The authors used a different set of material parameters which allows a linear limit for TE_0 branch. Since two different values of the propagation constants can exist for the same power level and power thresholds exist, this nonlinear layered structure is of potential interest as a lower threshold device and eventually, as an optical switch.

The authors used a different set of material parameters which allows a linear

limit for TE_0 branch. Since two different values of the propagation constants can exist for the same power level and power thresholds exist, this nonlinear layered structure is of potential interest as a lower threshold device and eventually, as an optical switch.

3.2. Nonlinear thin-film guided waves in saturable media

In what follows we will investigate the effect of saturation on the power-dependent wavevector and field distributions of nonlinear thin-film guided waves. We consider first a dielectric planar layered structure consisting of a linear substrate with dielectric constant ϵ_s in region I ($z < 0$), a linear dielectric film of thickness d and dielectric constant ϵ_f in region II ($0 < z < d$) and a nonlinear self-focusing cladding in region III ($z > d$) characterized by the dielectric tensor (2.19) where the parameter ϵ_{sat} is the maximum change in the dielectric function, i.e., $\epsilon \rightarrow \epsilon_c + \epsilon_{sat}$ for large field intensities.

For TE-polarized waves we have $\vec{E} = (0, E_y, 0)$ and E_y is a real quantity in the absence of loss. The Maxwell equations are:

$$\frac{d^2 E_y^I}{dz^2} - k_0^2 (\beta^2 - \epsilon_s) E_y^I = 0, \quad z < 0 \quad (3.106)$$

$$\frac{d^2 E_y^{II}}{dz^2} - k_0^2 (\beta^2 - \epsilon_f) E_y^{II} = 0, \quad 0 < z < d \quad (3.107)$$

$$\frac{d^2 E_y^{III}}{dz^2} - k_0^2 [\beta^2 - \epsilon_c - \epsilon_c^{NL}(E_y^{III})] E_y^{III} = 0, \quad z > d. \quad (3.108)$$

The first integrals of eqs. (3.106), (3.107) and (3.108) are:

$$\Phi_s = \left(\frac{dE_y}{dz} \right)^2 = k_0^2 (\beta^2 - \epsilon_s) E_y^2, \quad z < 0 \quad (3.109)$$

$$\Phi_f = \left(\frac{dE_y}{dz} \right)^2 = k_0^2 (\beta^2 - \epsilon_f) E_y^2 + C_f, \quad 0 < z < d. \quad (3.110)$$

$$\Phi_c = \left(\frac{dE_y}{dz} \right)^2 = k_0^2 \left[(\beta^2 - \epsilon_c) E_y^2 - \int_0^{E_y^2} \epsilon_c^{NL}(E_y^2) d(E_y^2) \right], \quad z > d, \quad (3.111)$$

where C_f is the integration constant.

For TE-polarized waves both the fields E_y and their derivatives $\frac{dE_y}{dz}$ are continuous across the interfaces $z = 0$ and $z = d$. Next we get the following relations between the integration constant C_f and the fields E_0 and E_d at the interfaces $z = 0$ and $z = d$, respectively:

$$\frac{C_f}{k_0^2} = (\epsilon_f - \epsilon_s) E_0^2 = (\epsilon_f - \epsilon_c) E_d^2 - \int_0^{E_d^2} \epsilon_c^{NL}(E_y^2) d(E_y^2). \quad (3.112)$$

Since $\frac{dE_y}{dz} = \Phi_f^{1/2}$ and taking into account that the integration over the film can be written as:

$$\int_{E_0}^{E_d} \frac{dE_y}{\Phi_f^{1/2}} = d \quad (3.113)$$

finally we obtain the dispersion relation for the TE_m waves /40/:

$$\text{tg}(k_0 q_f d) = \frac{q_f (q_s + \bar{q}_c)}{(q_f^2 - q_s \bar{q}_c)}, \quad (3.114)$$

Here $q_s = (\beta^2 - \epsilon_s)^{1/2}$, $q_f = (\epsilon_f - \beta^2)^{1/2}$, $\bar{q}_c = (-1)^M (\beta^2 - \epsilon_{cNL})^{1/2}$,

and

$$\epsilon_{cNL} = \epsilon_c + \frac{1}{E_d^2} \int_0^{E_d^2} \epsilon_c^{NL}(E_y^2) d(E_y^2). \quad (3.115)$$

We have $M_c = 1$ if a self-focused peak (real field maximum) occurs in the nonlinear cladding medium, otherwise $M_c = 0$ (virtual

field maximum). It is to be noted that when a peak occurs in the nonlinear cladding medium the field amplitude \bar{E}_y is evaluated from

$$\Phi_c(\bar{E}_y, \beta) = 0$$

For $\beta > n_f$ the dispersion relation is:

$$\text{th}(k_0 \tilde{q}_f d) = - \frac{\tilde{q}_f (q_s + \bar{q}_c)}{(\tilde{q}_f^2 + q_s \bar{q}_c)} \quad (3.116)$$

This dispersion relation has solution $\beta > n_f$ if and only if there is a real field maximum (self-focused peak) in the nonlinear cladding, i.e., $M_c = 1$ and $\bar{q}_c = -(\beta^2 - \epsilon_c n_c)^{1/2} Q$. If there is no self-focused peak in the cladding medium ($M_c = 0$), then we have $\bar{q}_c = q_c = [\varphi(u)]^{1/2}$, where $\varphi(u)$ is given by eqs. (2.32) or (2.33). Thus by using eqs. (3.112) and (3.113) we obtain:

$$P_s = \frac{1}{2} P_0 \beta \frac{u}{q_s} \frac{(q_c^2 + q_f^2)}{(q_s^2 + q_f^2)} \quad (3.117)$$

$$P_f = \frac{1}{2} P_0 \beta u \left[\kappa_0 d \frac{(q_c^2 + q_f^2)}{q_f^2} + \frac{q_c}{q_f^2} + \frac{q_s}{q_f^2} \frac{q_c^2 + q_f^2}{q_s^2 + q_f^2} \right] \quad (3.118)$$

$$P_c = \frac{1}{2} P_0 \beta \int_0^u \frac{dx}{[\varphi(x)]^{1/2}} \quad (3.119)$$

where $u = d_c E_d^2$.

In the case of a Kerr-law nonlinear cladding the integral (3.119) can be evaluated analytically and we get

$$P_c = 2 P_0 \beta \left[(\beta^2 - \epsilon_c + \frac{1}{2} u)^{1/2} - (\beta^2 - \epsilon_c)^{1/2} \right] \quad (3.120)$$

For a self-focusing cladding ($d_c > 0$), a field maximum can occur in that medium at sufficiently high powers, i.e., $M_c = 1$ and $\bar{q}_c = -q_c$, where $q_c = [\varphi(u)]^{1/2}$ with $\varphi(u)$ given by eqs. (2.32) and (2.33). In this case the results can be summarized in the form:

$$P_f = \frac{1}{2} P_0 \beta u \left[\kappa_0 d \frac{q_c^2 + q_f^2}{q_f^2} - \frac{q_c}{q_f^2} + \frac{q_s}{q_f^2} \frac{q_c^2 + q_f^2}{q_s^2 + q_f^2} \right] \quad (3.121)$$

$$P_c = \frac{1}{2} P_0 \beta \left[\int_0^u \frac{dx}{[\varphi(x)]^{1/2}} - \int_u^u \frac{dx}{[\varphi(x)]^{1/2}} \right] \quad (3.122)$$

and P_s is given by eq. (3.117).

For a Kerr-law self-focusing cladding the integrals in (3.122) can be evaluated analytically and we have

$$P_c = 2 P_0 \beta \left[(\beta^2 - \epsilon_c + \frac{1}{2} u)^{1/2} + (\beta^2 - \epsilon_c)^{1/2} \right] \quad (3.123)$$

For $\beta > n_f$ we finally obtain

$$P_s = \frac{1}{2} P_0 \beta \frac{u}{q_s} \frac{q_c^2 - \tilde{q}_f^2}{q_s^2 - \tilde{q}_f^2} \quad (3.124)$$

$$P_f = \frac{1}{2} P_0 \beta u \left[\frac{q_c}{q_f^2} - \kappa_0 d \frac{q_c^2 - \tilde{q}_f^2}{q_f^2} - \frac{q_s}{q_f^2} \frac{q_c^2 - \tilde{q}_f^2}{q_s^2 - \tilde{q}_f^2} \right] \quad (3.125)$$

and P_c is given by eq. (3.122).

We consider the case of liquid crystal MBBA ($n_c = 1.55$, $n_{2c} = 10^{-9} \text{ m}^2/\text{W}$) on a glass waveguide ($n_f = 1.57$, $d = 2 \mu\text{m}$) with a substrate chosen such that $n_s = n_c = 1.55$. We have performed numerical calculations of the effective index β as function of the total power flow P . The numerical results for TE-polarized waves guided by a planar layered structure with a nonlinear cladding described by the dielectric function (2.19) are shown in Fig. 15 for several dimensionless parameters ϵ_{sat} . It is to be noted that comparing to the Kerr-law case ($\epsilon_{\text{sat}} = \infty$) the characteristic behaviour of TE₀ and TE₁ nonlinear wave solutions are preserved provided that the saturable value $n_{\text{sat}} = (\epsilon_c + \epsilon_{\text{sat}})^{1/2} n_c$ is not too small (i.e., for $\epsilon_{\text{sat}} = 0.1256$ or $n_{\text{sat}} = 0.04$ in Fig. 15). The absolute maximum in the TE₁ guided wave power depends strongly on the saturation value and for n_{sat} too small (i.e., for $\epsilon_{\text{sat}} = 0.0155$ or $n_{\text{sat}} = 0.005$) no absolute limiting action is predicted. For the TE₀ branch the propagation constant β approaches the value $\beta = (\epsilon_c + \epsilon_{\text{sat}})^{1/2}$ asymptotically with power (see the curve corresponding to $\epsilon_{\text{sat}} = 0.1256$

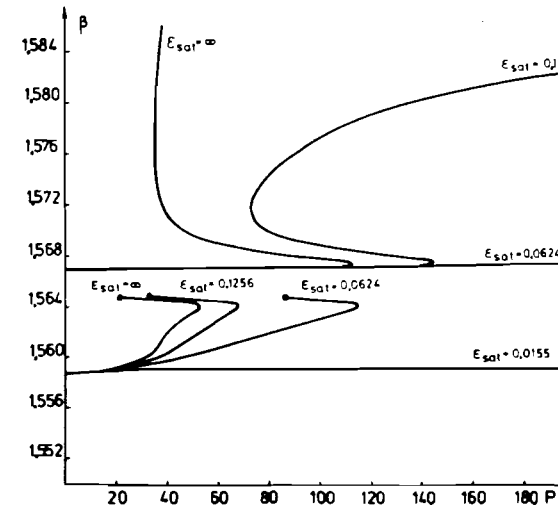


Fig. 15. The propagation constant β versus power P for a self-focusing cladding, where $\lambda = 0.515 \mu\text{m}$ (after /100).

in Fig. 15). Thus the characteristic features of the TE_m branches are retained provided that n_{sat} is much less than the low power refractive index differences ($n_f - n_c$) or ($n_f - n_s$). The important conclusion to be drawn from these calculations is that the saturation effects, if too large, can alter and in some cases eliminate the more interesting power-dependent features of nonlinear guided waves.

For two self-focusing saturable bounding media ($n_{2c} \neq n_{2s}$) the effects of saturation on the two separate (unconnected) TEO branches is quite dramatic (see /100/). In this case the switching characteristics are quite different when saturation is included in both the substrate and the cladding. This should be important for applications of nonlinear guided waves to all-optical switching devices.

We consider now a three layer asymmetric structure consisting of a linear substrate with dielectric constant ϵ_s , a thin dielectric film of thickness d with dielectric constant ϵ_f and a nonlinear self-defocusing ($d_c < 0$) cladding characterized by one of the two types of saturated nonlinearities:

$$\epsilon_{xx} = \epsilon_{yy} = \epsilon_{zz} = \epsilon_c - \epsilon_{sat} \left[1 - \exp\left(-\frac{|d_c| E_y^2}{\epsilon_{sat}}\right) \right] \quad (3.126)$$

$$\epsilon_{xx} = \epsilon_{yy} = \epsilon_{zz} = \epsilon_c - \frac{|d_c| E_y^2}{1 + \frac{|d_c| E_y^2}{\epsilon_{sat}}} \quad (3.127)$$

We remark that both dielectric tensors (3.126) and (3.127) are Kerr-like, i.e., $\epsilon \rightarrow \epsilon_c - |d_c| E_y^2$ for small field intensities and reveal a common saturable level $(\epsilon_c - \epsilon_{sat})$. In the case of a self-defocusing cladding the field pattern reveals a virtual field maximum in the nonlinear cladding ($M_c = 0$) and the dispersion relation is

$$\text{tg}(k_0 q_f d) = \frac{q_f (q_s + q_c)}{q_f^2 - q_s q_c} \quad (3.128)$$

where $q_c = [\varphi(u)]^{1/2}$, $u = |d_c| E_d^2$ and

$$\varphi(u) = \beta^2 \epsilon_c + \epsilon_{sat} - \frac{\epsilon_{sat}^2}{u} \left[1 - \exp\left(-\frac{u}{\epsilon_{sat}}\right) \right] \quad (3.129)$$

$$\varphi(u) = \beta^2 \epsilon_c + \epsilon_{sat} - \frac{\epsilon_{sat}^2}{u} \ln\left(1 + \frac{u}{\epsilon_{sat}}\right) \quad (3.130)$$

corresponding to the dielectric tensor (3.126) and (3.127), respectively.

The total power flow is $P = P_s + P_f + P_c$, where P_s , P_f and P_c are given by eqs. (3.117), (3.118), and (3.119). We have performed numerical calculations of the effective index β as function of the total power flow P for several dimensionless parameters ϵ_{sat} . The numerical results for TE waves guided by a multiple quantum well (MQW) GaAl_xAs_{1-x} structure are shown in Fig. 16 for both dielectric functions (3.126) and (3.127). For Kerr-law ($\epsilon_{sat} = \infty$) self-defocusing cladding with $n_c > n_s$ there is a maximum in the power which can be transmitted. For a realistic saturable nonlinear cladding, optical

limiting occurs, provided that $n_{sat} = n_c - (\epsilon_c - \epsilon_{sat})^{1/2}$ is large enough (see Fig. 16 for $\epsilon_{sat} = 0.0676$, i.e., $n_{sat} = 0.01$).

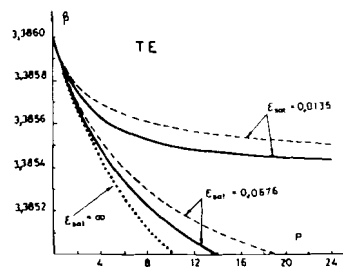


Fig. 16.

Effective index β versus power P for a self-defocusing cladding. Here $n_f = 3.390$, $n_c = 3.385$, $n_s = -2 \times 10^{-9}$ m²/W, $n_s = 3.380$, $d = 1.07 \mu\text{m}$, $\lambda = 0.82 \mu\text{m}$. Solid and dashed lines correspond to dielectric tensors (2.19) and (2.20), respectively.

We see from Fig. 16 that for a self-defocusing cladding medium the effective index β decreases monotonically with guided wave power and for $n_c > n_s$ cutoff occurs at a finite power. This phenomenon can be used for upper threshold optical devices in which the cutoff power can be tuned, for example, by using a thin film of bulk GaAl_xAs_{1-x} with variable refractive index $n_f(x)$ /58/.

3.3. Stability to propagation of nonlinear slab-guided waves

The question of stability to propagation of various TEM nonlinear guided wave solutions has only recently been studied by numerical techniques /44,46-50/. Analytical stability analysis is complicated by the fact that the system under study is of Hamiltonian form (see /44/). As the eigenvalues of the linearized system all lie on the imaginary axis the usual stability arguments associated with the dissipative systems do not apply (unless one deliberately introduces losses into the system).

We treat first the specific case of a TE-polarized guided wave in a symmetric nonlinear planar waveguide consisting of a linear guiding film with refractive index n_f bounded on both sides by identical self-focusing Kerr-law cladding and substrate layers, i.e., $n_c = n_s$ and $n_{2c} = n_{2s}$ (see Fig. 17a). The dependence of the power flow P on the propagation constant β is shown in Fig. 17b for a symmetric layered structure with the following parameters: $n_c = n_s = 1.5$, $n_f = 2$, $d/\lambda = 0.4$. In Fig. 18 we present the results of the evolution of the field distribution with propagation distance taking as initial data the electric field distribution immediately before and after the bifurcation point on the symmetric TEO branch (S).

At $\beta = 1.89 < \beta_c$ the symmetric wave is stable to propagation over at least 180 wavelengths (see Fig. 18a) while at $\beta = 1.90 > \beta_c$ the S-

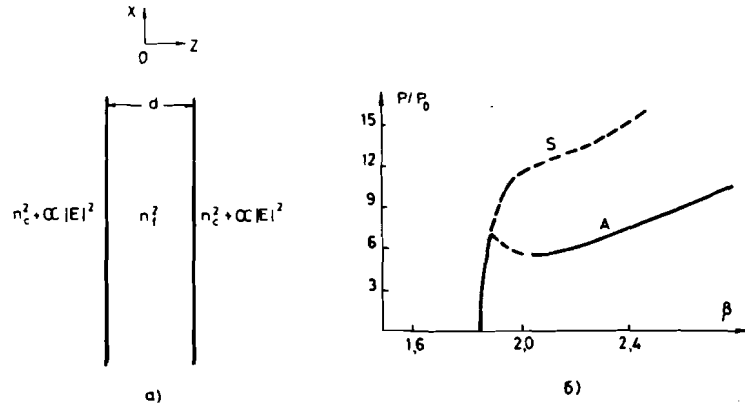


Fig. 17. a) Sketch of the planar waveguide geometry; b) Nonlinear dispersion curves for a symmetric planar waveguide. Here $n_f=2.0$, $n_c=n_s=1.5$, $d/\lambda=0.4$. The curves are marked as follows: S - for symmetric wave, A - for asymmetric wave. Beyond bifurcation point $\beta=\beta_c \approx 1.89$ both branches (S and A) are unstable (dashed line). The doubly degenerate A-wave becomes stable on the positively sloped region (after /44/).

wave breaks symmetry after only 18 wavelengths (see Fig. 18b). In this case the wave starts to drive into either the substrate and cladding layers. Therefore the symmetric TE₀ branch (S) loses stability on the positively sloped branch of the dispersion curve (see Fig. 18b) at the bifurcation point (critical propagation constant $\beta=\beta_c \approx 1.89$) where the double degenerate asymmetric wave A appears /44/.

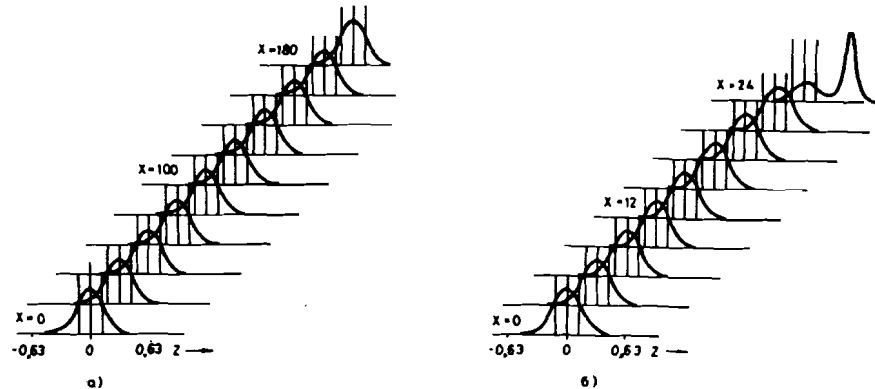


Fig. 18. Evolution of the field distribution with propagation distance for the symmetric wave (S) just below a) $\beta=1.89$ and beyond b) $\beta=1.90$ bifurcation point $\beta=\beta_c$ (after /44/).

Next we consider an asymmetric three layer planar structure consisting of a linear substrate with dielectric constant $\epsilon_s=n_s^2$ in region I ($z < 0$), a thin dielectric film of thickness d with dielectric constant $\epsilon_f=n_f^2$ in region II ($0 < z < d$) and a nonlinear self-focusing cladding characterized by the diagonal dielectric tensor (2.19) or (2.20) in region III ($z > d$). The TE-polarized wave of frequency ω propagates along the x -axis and the electric field is homogeneous in the y direction (z being the transverse coordinate). The only nonvanishing component of the electric field $E_y(\vec{r}, t)$ is given by eq. (2.11). Then in the usual slowly varying envelope approximation we obtain the following equation for the amplitude $A(x, z) = \alpha_c^{1/2} E_y(x, z)$

$$-2i\beta\kappa_0 \frac{\partial A}{\partial x} = \frac{\partial^2 A}{\partial z^2} - \gamma^2(z)\kappa_0^2 A + \Theta(z)\kappa_0^2 f(|A|^2)A. \quad (3.131)$$

Here $\Theta(z) = 0$ for $-\infty < z < d$ and $\Theta(z) = 1$ for $z > d$; $\gamma^2(z) = \beta^2 - n_s^2$

for $z < 0$, $\gamma^2(z) = \beta^2 - n_f^2$ for $0 < z < d$, $\gamma^2(z) = \beta^2 - n_c^2$ for $z > d$ and

$$f(|A|^2) = \epsilon_{sat} \left[1 - \exp\left(-\frac{|A|^2}{\epsilon_{sat}}\right) \right] \quad (3.132)$$

$$f(|A|^2) = \frac{|A|^2}{\left(1 + \frac{|A|^2}{\epsilon_{sat}}\right)} \quad (3.133)$$

corresponding to the dielectric functions (2.19) and (2.20), respectively. Note that for a Kerr-law medium we have $f(|A|^2) = |A|^2$.

The parabolic equation (3.131) is a complicated mixed type linear/nonlinear Schrödinger-like equation. The x -independent solution of eq. (3.131), i.e., $A(x, z) = A_0(z)$ represents stationary nonlinear guided waves whose effective index β is subject to a nonlinear dispersion relation $\beta = \beta(P)$, where P is the power flow. Equation (3.131) has two integrals of motion: $I(\beta)$ given by eq. (2.39) and

$$H(\beta) = \kappa_0 \int_{-\infty}^{\infty} \left\{ \left| \frac{\partial A}{\partial z} \right|^2 + \kappa_0^2 \gamma^2(z) |A|^2 - \kappa_0^2 \Theta(z) g(|A|^2) \right\} dz. \quad (3.134)$$

Here we have

$$g(|A|^2) = \int_0^{|A|^2} f(|A|^2) d(|A|^2), \quad (3.135)$$

when $f(|A|^2)$ is given by eqs. (3.132) or (3.133). For Kerr-law media we obtain $g(|A|^2) = \frac{1}{2}|A|^4$ and for saturable media $g(|A|^2)$ has the following expressions

$$g(|A|^2) = \frac{1}{2} \epsilon_{sat} \left[1 - \exp\left(-\frac{|A|^2}{\epsilon_{sat}}\right) \right] |A|^2 \quad (3.136)$$

$$g(|A|^2) = \frac{1}{2} \epsilon_{sat} \left[\ln\left(1 + \frac{|A|^2}{\epsilon_{sat}}\right) \right] |A|^2 \quad (3.137)$$

corresponding to the dielectric functions (2.19) and (2.20), respectively. Note that for arbitrary solutions of eq. (3.131) we thus have $dI/dx=0$ and $dH/dx=0$.

The stability of the stationary nonlinear thin-film guided waves was investigated numerically. For the difference approximation of eq. (3.131) we used the Crank-Nicolson scheme. The corresponding system of nonlinear equations was solved on the successive steps in x by Newton method combined with a matrix tridiagonal inversion along Z . We have chosen the grid sizes equal in magnitude $k_0 \Delta x = k_0 \Delta z = 0.4$. This difference scheme makes it possible to conserve the integrals of motion $I(\beta)$ and $H(\beta)$ on the grid. The conservation of the total power flow $P(\beta)$ was always better than 99%. Unstable stationary waves are defined as waves whose field distribution along the depth coordinate x changes with propagation distance z . Otherwise, the stationary solution is called stable.

For a Kerr-law nonlinear cladding the stationary wave is unstable on the negatively sloped region of the nonlinear dispersion curve $\beta = \beta(P)$ and starts to drift into the nonlinear medium. In this case the emission of a single soliton, i.e., a self-focused channel (see Fig. 19) was found to be a route by which unstable nonlinear guided waves decay /47,49,52/.

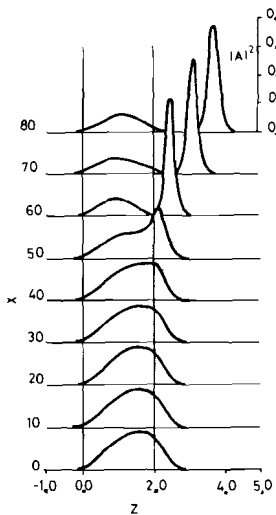


Fig. 19.

Evolution of the TEO nonlinear guided wave field distribution with propagation distance for a Kerr-law cladding. The initial field pattern $A_0(z)$ corresponds to $\beta=1.5685$.

In a case of a nonlinear saturable cladding described by the dielectric tensor (2.19) with $\epsilon_{sat}=0.1256$, the TEO wave on the negatively sloped branch of the nonlinear dispersion curve (see Fig.15) is unstable /50/. Numerical propagation over the first 400 wavelengths is shown in fig. 20 for $\beta=1.5685$.

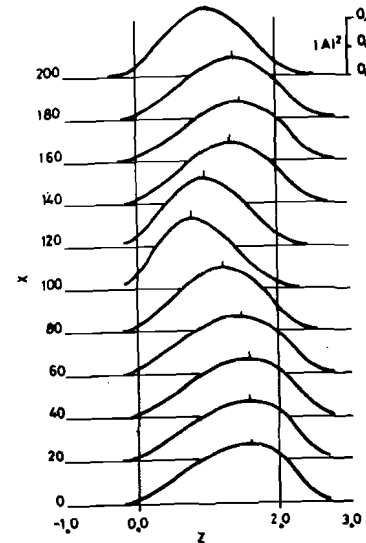


Fig. 20.

Evolution of the TEO nonlinear guided wave field distribution with propagation distance for a saturable cladding described by the dielectric function (2.19) with $\epsilon_{sat}=0.1256$.

In this case the instability is weak, the field remains confined to the wave-guiding film and the field maximum oscillates aperiodically back and forth between the film boundaries. The evolution of the TEO nonlinear guided wave field distribution with propagation distance for the case of a saturable cladding described by the dielectric tensor (2.19) with $\epsilon_{sat}=0.1256$ is shown in Fig. 21 for $\beta=1.58$ on the positively sloped branch of the nonlinear dispersion curve $\beta = \beta(P)$. For this value of the effective index the nonlinear stationary wave $A_0(z)$ is stable to propagation (see Fig. 21). Numerical propagation of the stationary wave confirms that the TEO nonlinear guided wave in an asymmetric layered structure in which self-focusing occurs in only one of the two boundary media is stable on the positively sloped branch of the nonlinear dispersion curve /52/.

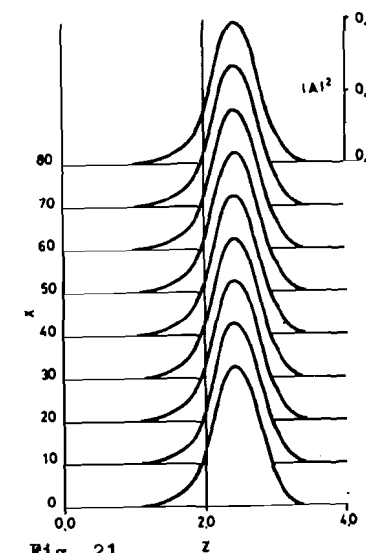


Fig. 21.

The same as Fig. 20, but for $\beta=1.58$.

the positively sloped branch of the nonlinear dispersion curve $\beta = \beta(P)$. For this value of the effective index the nonlinear stationary wave $A_0(z)$ is stable to propagation (see Fig. 21). Numerical propagation of the stationary wave confirms that the TEO nonlinear guided wave in an asymmetric layered structure in which self-focusing occurs in only one of the two boundary media is stable on the positively sloped branch of the nonlinear dispersion curve /52/.

In the presence of dissipation, the Kramers-Kronig relation dictates that at least linear absorption must accompany nonlinear refraction. Therefore, we must include in eq. (3.131) an absorptive term:

$$-2i\beta k_0 \frac{\partial A}{\partial x} = \frac{\partial^2 A}{\partial z^2} - \gamma^2(z) k_0^2 A + \Theta(z) k_0^2 f(|A|^2) A + i\beta k_0^2 \Gamma(z) A, \quad (3.138)$$

where $\Gamma(z)$ is the absorption profile.

The effects of linear absorption on TEo nonlinear guided waves in an asymmetric waveguide with a Kerr-law cladding have been investigated in /55/ by using the beam propagation method /101,102/. It was shown that is preferable to fabricate nonlinear asymmetric optical waveguides with lower absorption in the waveguiding film. It is of interest to mention that the beam propagation method (incorporating a split-step fast Fourier transform) provides a unified treatment of various guided and radiation field problems subjected to paraxiality.

4. Transverse Electric Polarized Nonlinear Surface Plasmon Polaritons

4.1. Kerr-law bounding media

In the last years considerable interest has been raised in the theoretical /78,79/ and experimental /103,104/ study of surface polaritons. As is well known the boundary between two linear dielectric media cannot support a TE-polarized surface polariton. However, if one or both of the media exhibit an intensity-dependent refractive index, it has been predicted (see /15,18,20,60/) that TE-polarized surface polariton should exist at powers exceeding a threshold value.

Additionally to the well-investigated nonlinear guided waves which can be supported by a linear dielectric film surrounded by at least one medium (cladding or substrate) with an intensity-dependent refractive index new waves have also been predicted for metal films bounded on one of both sides by nonlinear media /105-108/. Nonlinear TE-polarized waves guided by very thin metal films surrounded on both sides by nonlinear media exist only for power levels above a threshold that depends on the material parameters (see /106/). Lederer and Michalache /107/ demonstrated that nonlinear TE-polarized surface plasmon polaritons also exist in planar configurations with either a nonlinear cladding or a nonlinear substrate. For this asymmetric layered structure the nonlinear dispersion curves exhibit a definite power threshold and a limited range for the permitted propagation constants as well.

In what follows we will investigate the characteristics of nonlinear TE-polarized waves guided by an asymmetric three-layer configuration consisting of a linear substrate with dielectric constant ϵ_s in region I ($z < 0$), a very thin metal film with dielectric constant $\epsilon_f = -|\epsilon_f| < 0$ in region II ($0 < z < d$) and a nonlinear self-focusing Kerr-law cladding in region III ($z > d$). The field distribution in the substrate, film and cladding regions, respectively is given by:

$$E_y^I(z) = E_0 \exp(\kappa_0 q_s z) \quad , \quad z < 0 \quad (4.1)$$

$$E_y^{II}(z) = E_0 \left[\frac{q_s + \tilde{q}_f}{2\tilde{q}_f} \exp(\kappa_0 \tilde{q}_f z) + \frac{\tilde{q}_f - q_s}{2\tilde{q}_f} \exp(-\kappa_0 \tilde{q}_f z) \right] \quad (4.2)$$

$0 < z < d$

$$E_y^{III}(z) = \left(\frac{2}{\alpha_c}\right)^{1/2} q_c \left\{ \text{ch}[\kappa_0 q_c (z - z_c)] \right\}^{-1} \quad , \quad z > d, \quad (4.3)$$

where $q_s = (\beta^2 - \epsilon_s)^{1/2}$, $\tilde{q}_f = (\beta^2 + |\epsilon_f|)^{1/2}$ and $q_c = (\beta^2 - \epsilon_c)^{1/2}$. Here the surface field E_0 is given by

$$\alpha_c E_0^2 = 2 \left\{ 1 - \text{th}^2[\kappa_0 q_c (z_c - d)] \right\} \left[\text{ch}(\kappa_0 \tilde{q}_f d) + \frac{q_s}{\tilde{q}_f} \text{sh}(\kappa_0 \tilde{q}_f d) \right]^{-2} \quad (4.4)$$

As a result of the continuity requirements of E_y and dE_y/dz at the interfaces $z = 0$ and $z = d$ the effective index β is subject to a dispersion relation

$$\text{th}(\kappa_0 \tilde{q}_f d) = \frac{\tilde{q}_f \left\{ q_c \text{th}[\kappa_0 q_c (z_c - d)] q_s \right\}}{\left\{ \tilde{q}_f^2 - q_s q_c \text{th}[\kappa_0 q_c (z_c - d)] \right\}} \quad (4.5)$$

This dispersion relation has a solution if and only if $n_s > n_c$ and $z_c > d$, i.e., a field maximum must always be situated within the cladding region. The power per unit distance along the wavefront carried by the wave is given by

$$P_s = \frac{1}{2} P_0 \beta \frac{\alpha_c \bar{E}_0^2}{q_s} \quad (4.6)$$

$$P_f = \frac{1}{2} P_0 \beta \alpha_c E_0^2 \left\{ \kappa_0 d \left(1 - \frac{q_s^2}{\tilde{q}_f^2} \right) + \frac{1}{\tilde{q}_f} \text{sh}(\kappa_0 \tilde{q}_f d) \times \right. \quad (4.7)$$

$$\left. \times \left[\left(1 + \frac{q_s^2}{\tilde{q}_f^2} \right) \text{ch}(\kappa_0 \tilde{q}_f d) + 2 \frac{q_s}{\tilde{q}_f} \text{sh}(\kappa_0 \tilde{q}_f d) \right] \right\}$$

$$P_c = \frac{1}{2} P_0 \beta q_c \left\{ 1 + \text{th}[\kappa_0 q_c (z_c - d)] \right\} \quad (4.8)$$

where $P_0 = (2\alpha_c \kappa_0)^{-1} (\epsilon_0 / \mu_0)^{1/2}$,

The numerical calculations were performed with the following parameters: $n_c = 1.55$, $n_{zc} = 10^{-9} \text{ m}^2/\text{W}$, $\epsilon_f = -10$ and $\lambda = 0.515 \mu\text{m}$ (argon ion laser).

The dependence of the propagation constant β on the guided wave power P is shown in Fig. 22 for different refractive indices of the substrate (see /107/). As in the symmetrical configuration studied in

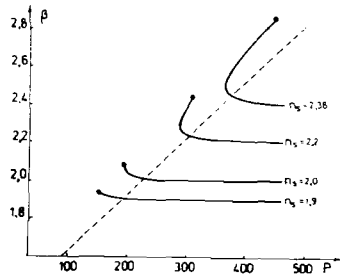


Fig. 22.

Propagation constant β versus guided wave power for $n_c=1.55$, $n_{2c}=10^{-9}$ m^2/W , $\epsilon_f = -10$, $\lambda=0.515 \mu m$ and $d=0.005 \mu m$. Solid curves: n_s indicated at the curves and $n_{2s}=0$. Dashed curve: $n_s = n_c = 1.55$, $n_{2s} = n_{2c} = 10^{-9}$ m^2/W .

/106/ we found a definite power threshold where the nonlinear TE-polarized surface plasmon polaritons start. This threshold increases with the

refractive index of the substrate. The dashed curve in Fig. 22 corresponds to the symmetrical planar structure with the following material parameters: $n_s = n_c = 1.55$, $n_{2s} = n_{2c} = 10^{-9}$ m^2/W . We see from Fig. 22 that in the case of an asymmetrical configuration with $n_s > n_c$ and $n_{2s} = 0$, two different values of the propagation constant correspond to the same value of the control parameter P and an upper β -limit occurs additionally to the lower one which is determined by n_s . The upper β -limit is due to the impossibility of field matching at the metal film-dielectric substrate interface. The field distribution for β near its lower limit n_s shows that the electric field penetrates deep into the substrate region and for β approaching the upper limit the field energy is mainly concentrated within the nonlinear cladding which is favourable for diminishing absorption losses in realistic metal films. So, a possible switching between the upper and the lower branch of the dispersion curve is accompanied by a transition from a high transmission state to a low one.

4.2. Non-Kerr-like bounding media

We consider an asymmetrical configuration consisting of a linear dielectric substrate with dielectric constant ϵ_s , a thin metal film of thickness d with dielectric constant $\epsilon_f = -|\epsilon_f| < 0$ and a nonlinear self-focusing cladding characterized by one of the dielectric tensors (2.19), (2.20) and (2.21). We use the formalism developed in /40/ to investigate the power dependence of the effective index for both saturable and power-law dielectric tensors (non-Kerr-like media).

The dispersion relation of nonlinear TE-polarized surface plasmon polaritons is given by

$$\text{th}(\kappa_0 \tilde{q}_f d) = \frac{\tilde{q}_f (q_c - q_s)}{\tilde{q}_f^2 - q_s q_c}, \quad (4.9)$$

where $\tilde{q}_f = (\beta^2 + |\epsilon_f|)^{1/2}$, $q_s = (\beta^2 - \epsilon_s)^{1/2}$, $q_c = [\varphi(u)]^{1/2}$, $u = \alpha_c E_d^2$, where E_d is the electric field at the interface $z=d$ and $\varphi(u)$ is given by eqs. (2.32), (2.33) and (2.34). The dispersion relation (4.9) has solution $\beta > n_s$, if and only if $n_s > n_c$ and in this case a field maximum (self-focused peak) must be situated within the self-focusing cladding medium. The total power flow per unit length is $P = P_s + P_f + P_c$ where P_c is given by eq. (3.122) and P_s and P_f are given by eqs. (3.124) and (3.125), respectively.

The numerical calculations were performed with the following parameters: $n_c = 1.55$, $n_{2c} = 10^{-9}$ m^2/W (liquid crystal MBBA), $\epsilon_f = -10$, $n_s = 1.6$, $d = 10^{-3}$ μm and $\lambda = 0.515 \mu m$. The β -power plots for the case of a self-focusing cladding characterized by the dielectric tensors (2.19), (2.20) and (2.21) are shown in Fig. 23. As in the symmetrical configuration studied in /106/ we found a definite power threshold where nonlinear TE-polarized surface plasmon polaritons start. The upper β -limit that occurs additionally to the lower one ($\beta = n_s$) is determined from $u = \alpha_c E_d^2 = 0$, i.e., $P_s = P_f = 0$ and $P_c \neq 0$ (see termination points A, B in Fig. 23).

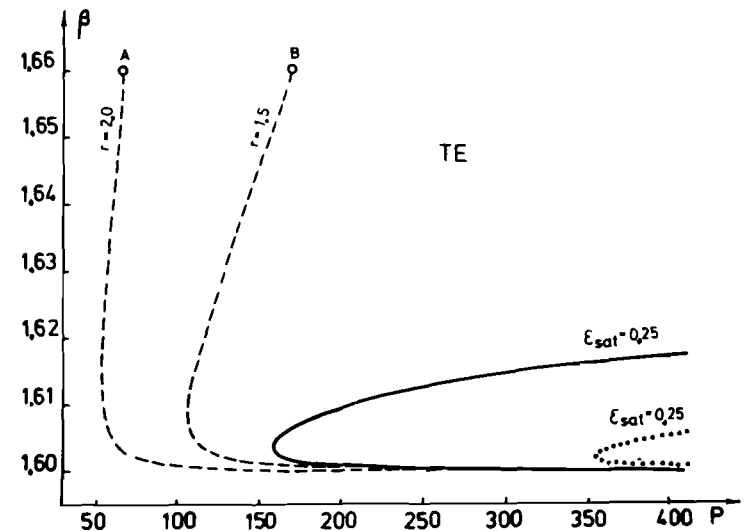


Fig. 23. The dependence of the effective index β on the guided wave power P for $n_c=1.55$, $n_{2c}=10^{-9}$ m^2/W , $n_s=1.6$, $\epsilon_f=-10$, $d=10^{-3}$ μm , $\lambda=0.515 \mu m$, $\alpha_c = 1.75 \times 10^{-9}$ $(m/V)^{1.5}$ ($\nu=1.5$) and $\alpha_c = 6.4 \times 10^{-12}$ $(m/V)^2$ ($\nu=2.0$). Solid and dotted lines correspond to dielectric tensors (2.10) and (2.20), respectively. Dashed lines correspond to a power-law cladding with the exponent $\nu=1.5$ and $\nu=2.0$.

For effective index β approaching the upper value, the optical field will mainly be concentrated within the nonlinear self-focusing cladding. We see from Fig. 2J that the minimum power required for the excitation of nonlinear TE-polarized surface plasmon polaritons increases with decreasing ϵ_{sat} . Furthermore, the effective index β approaches its limiting value of $(\epsilon_c + \epsilon_{sat})^{1/2}$ asymptotically with increasing power. The conclusion to be drawn from these calculations is that the saturation effects can alter the specific power-dependent features of nonlinear TE-polarized surface plasmon polaritons in configurations with Kerr-law media. It should be noted that the combination of the very thin metal film thickness required, the losses usually associated with surface plasmon for small $|\epsilon_f|$ and the large changes in refractive index required will probably make such nonlinear waves difficult to observe experimentally.

5. Conclusions

We have shown in this review article that the use of media with nonlinear refractive indices enriches considerably the phenomenon of guided wave propagation in planar structures. Thus if one or more of the media bounding a dielectric or metal film exhibits an intensity-dependent refractive index, the number of nonlinear guided wave solutions, the propagation wavevector, the field distributions, the attenuation coefficient and the waveguide cut-off and cut-on conditions all become power-dependent. We have discussed a number of potential applications to all-optical signal processing of nonlinear guided wave phenomena in planar structures. Planar optical waveguides are primarily of interest for serial, rather than parallel processing systems.

The power-dependent field patterns can be used for switching and thresholding operations in a waveguide context whereas the power-dependent wavevector used in conjunction with a distributed coupler can lead to devices such as optical limiters, etc. We have shown that lower threshold devices that only pass optical pulses above a threshold power are possible based on self-focusing nonlinearities. Thus a planar optical waveguide with a nonlinear self-focusing cladding and a linear waveguiding film whose thickness is less than the TE₀ cut-off thickness at low power, can become transmitting at high power levels. Nonlinear guided wave limiters can be obtained if one or both of the media bounding the waveguiding film are characterized by a self-defocusing nonlinearity. Optical switching action can potentially be achieved if both the cladding and substrate media exhibit self-

focusing nonlinearities. Moreover a combination of controllable thresholding and limiting actions can be used to fix a range of power levels transmitted down by the nonlinear optical waveguide. Furthermore, the same type of phenomena should occur in channel waveguide which would reduce the waveguide volume and power operating levels considerably. For example, since most materials exhibit the saturated change in the refractive index Δn_{sat} in the range of 10^{-2} to 10^{-4} , power limiting action in the range of a few milliwatts would be expected for 1 mm wide light beam propagating in a planar waveguide. If one can extrapolate linearly with waveguide width to channel waveguides, then by using nonlinear guided waves, optical limiting action might be obtained at a few microwatts power levels.

Materials in general limit the experimental realizations of all the nonlinear guided wave phenomena predicted to date. The fact that the refractive index differences $n_f - n_c$ and $n_f - n_s$ which exist at low powers between the film and the bounding media must be less than the saturated change in the refractive index Δn_{sat} puts severe limitations on the material combinations which can be used for making a nonlinear planar optical waveguide. There is a need for new materials with optical nonlinearities n_{2f} greater than $10^{-13} \text{ m}^2/\text{W}$ and with attenuation coefficients less than 1 cm^{-1} in waveguide formats. The optical nonlinearities should be large enough that the various nonlinear devices can be implemented at milliwatt power levels. Since the nonlinear waveguide phenomena will be used primarily for serial signal processing, it is also necessary that, once the optical signal is turned off, the nonlinearly induced polarization should relax in the picoseconds range (the "turn-on" of the nonlinearities is usually instantaneous). Some candidate materials for nonlinear third order integrated optics devices such as GaAs/GaAlAs multiple quantum well structures, semiconductor doped glasses and nonlinear organic media (for example, polydiacetylene films) satisfy the above criteria although not all optimally. We look forward over the next few years to both the demonstration of more all-optical signal processing operations using currently available materials and to the development and utilization of new highly nonlinear materials with response time in the picoseconds range which will lead to many nonlinear guided wave devices for optical logic and signal processing.

Acknowledgements

It is a pleasure to thank V.G.Kadyshevski, P.N.Bogolyubov, M.Ivascu, I.I.Popescu, I.M.Popescu and I.Urau for continuous support and valuable encouragements.

References

1. Gibbs H.M., McCall S.L., Venkatesan T.N.K., Gossard A.C., Passner A., Wiegmann W. Appl.Phys.Lett., 1979, v. 35, p. 451-453.
2. Miller D.A.B., Smith S.D., Johnston A. Appl.Phys.Lett., 1979, v. 35, p. 658-660.
3. Lugiato L.A. Theory of optical bistability, in: Progress in Optics, 1984, v. 21, ed. E.Wolf (North-Holland, Amsterdam), p. 71.
4. Gibbs H.M., Mandel P., Peyghambarian N., Smith S.D. Optical Bistability III, Proc.Topical Meeting, Tucson, 1985, (Springer, Berlin, 1986).
5. Seaton C.T., Smith S.D., Tooley F.A.P., Prise M.E., Taghizadeh M.R. App.Phys.Lett., 1983, v. 42, p. 131-133.
6. Jewell J.L., Rushford M.C., Gibbs H.M. Appl.Phys.Lett., 1984, v. 44, p. 172-174.
7. Kogelnik H. Integrated optics, ed. T.Tamir (Springer, Berlin, 1975).
8. Sipe J.E., Stegeman G.I. J.Opt.Soc.Am., 1979, v. 69, p. 1976
9. Stegeman G.I., I.E.E.E.J. Quantum Electron., 1982, v. 18, p. 1610
10. Chen Y.J., Carter G.M. Appl.Phys.Lett., 1982, v. 41, p. 309-309.
11. Valera J.D., Seaton C.T., Stegeman G.I., Shoemaker R.L. et al. Appl.Phys.Lett., 1984, v. 45, p. 1013-1015.
12. Jensen S.M. I.E.E.E.J. Quantum Electron, 1982, v. 18, p. 1580
13. Cada M., Gauthier R.C., Paton B.E., Chrostowski J. Appl.Phys. Lett., 1986, v. 49, p. 755-757.
14. Seaton C.T., Xu Mai, Stegeman G.I., Winful H.G. Opt.Eng., 1985, v. 24, p. 593-599.
15. Литвак А.Г., Миронов В.А. Изв. ВУЗ, 1968, Радиофизика, т. II, с. I911-I912.
16. Miyagi M., Nishida S. Sci.Rep.Tohoku Univ., 1972, B24, p. 53
17. Каплан А.Е. Письма ЖЭТФ, 1976, т. 24, с. I32-I37.
18. Tomlinson W.J. Opt.Lett., 1980, v. 5, p. 323
19. Агранович В.М., Бабиченко В.С., Черняк Я. Письма ЖЭТФ, 1980, т. 32, с. 532-535.
20. Maradudin A.A. Z.Phys., 1981, B41, p. 341-344.
21. Ломтев А.И. Письма ЖЭТФ, 1981, т. 34, с. 64-67.
22. Fedyanin V.K., Mihalache D. JINR, E-17-81-137, Dubna, 1981, 4 p.
23. Ахмедиев Н.Н. ЖЭТФ, 1982, т. 83, с. 545-553.
24. Fedyanin V.K., Mihalache D. Z.Phys. B, 1982, v. 47, p. 167-173.
25. Lederer F., Langbein U., Ponath H.E. Appl.Phys. B., 1983, v. 31, p. 69
26. Lederer F., Langbein U., Ponath H.E. Appl.Phys. B, 1983, v. 31, p. 187
27. Yu M.Y. Phys.Rev. A, 1983, v. 28, p. 1855-1856.
28. Boardman A., Egan P. J.Phys.Colloq. C, 1984, v. 5, p. 291
29. Boardman A., Egan P. Phil.Trans.Roy.Soc.Lond. A, 1984, v. 313, p. 363
30. Stegeman G.I., Seaton C.T., Chilwell J., Smith S.D. Appl. Phys.Lett., 1984, v. 44, p. 830-832.
31. Mihalache D., Nazmitdinov R.G., Fedyanin V.K. Phys.Scripta, 1984, v. 29, p. 269-275.
32. Sibilia C., Bertolotti M., Sette D. Phil.Trans.Roy.Soc. Lond. A, 1984, v. 313, p. 361-362.
33. Leung K.M. Phys.Rev. A, 1985, v. 31, p. 1189-1192.
34. Leung K.M. Phys.Rev. B, 1985, v. 32, p. 5093-5101.
35. Stegeman G.I., Seaton C.T. J.Appl.Phys., 1985, v. 58, R 57 - R 78.
36. Михалаче Д., Федянин В.К. Краткие сообщения ОИЯИ, 1985, № 6, с. 5-10.
37. Mihalache D., Mazilu D. Appl.Phys. B, 1985, v. 37, p. 107
38. Mihalache D., Mazilu D. Appl.Phys. B, 1986, v. 41, p. 119
39. Mihalache D., Stegeman G.I., Seaton C.T., Wright E.M. et al. Opt.Lett., 1987, v. 12, p. 187-189.
40. Langbein U., Lederer F., Ponath H.E. Opt.Comm., 1985, v. 52, p. 417-420.
41. Stegeman G.I., Ariyasu J., Seaton C.T., Shen T.P., Moloney J.V. Appl.Phys.Lett., 1985, v. 47, p. 1254-1256.
42. Mihalache D., Mazilu D. Solid St.Comm., 1986, v. 60, p. 397-399.
43. Ахмедиев Н.Н., Корнеев В.И., Кузьменко Ю.В. ЖЭТФ, 1985, т. 88, с. I07-II5.
44. Jones C.K.R.T., Moloney J.V. Phys.Lett. A, 1986, v. 117, p. 175-180.
45. Ariyasu J., Seaton C.T., Stegeman G.I., Moloney J.V. I.E.E.E.J., Quantum Electron, 1986, v. 22, p. 984-987.
46. Moloney J.V., Ariyasu J., Seaton C.T., Stegeman G.I. Appl.Phys. Lett., 1986, v. 48, p. 826-828.
47. Moloney J.V., Ariyasu J., Seaton C.T., Stegeman G.I. Opt.Lett., 1986, v. 11, p. 315.
48. Leine L., Wachter Ch., Langbein U., Lederer F. Opt.Lett., 1986, v. 11, p. 590-593.
49. Mihalache D., Mazilu D. Solid St.Comm., 1987, v. 63, p. 215-217.

50. Mihalache D., Mazilu D. Phys.Lett. A, 1987, v. 122, p. 381-384.
51. Wright E.M., Stegeman G.I., Seaton C.T., Moloney J.V. Appl.Phys.Lett., 1986, v. 49, p. 435-436.
52. Wright E.M., Stegeman G.I., Seaton C.T., Moloney J.V., Boardman A.D. Phys.Rev. A, 1986, v. 34, p. 4442-4444.
53. Розанов Н.Н. Опт. спектроскопия, 1979, т. 47, с. 606-609.
54. Tomlinson W.J., Gordon J.P., Smith P.W., Kaplan A.E. Appl.Opt., 1982, v. 21, p. 2041-2051.
55. Gubbels M., Wright E.M., Stegeman G.I., Seaton C.T., Moloney J.V. Opt.Comm., 1987, v. 61, p. 357-362.
56. Vach H., Seaton C.T., Stegeman G.I., Khoo I.C. Opt.Lett., 1984, v. 9, p. 238-240.
57. Bennion I., Goodwin M.J., Stewart W.J. Electron Lett., 1985, v. 21, p. 41.
58. Stegeman G.I., Seaton C.T., Hetherington III, Boardman A.D., Egan P. Nonlinear Optics: Material and Devices eds. C.Flytzanis and J.L.Oudar (Springer, Berlin, 1986).
59. Maker P.D., Terhune R. Phys.Rev. A, 1964, v. 137, p. 801-818.
60. Maradudin A.A. Optical and Acoustic Waves in Solids: Modern Topics ed. Borissov M. (World Scientific, Singapore, 1983), p. 72.
61. Каплан А.Е. ЖЭТФ, 1977, т. 72, с. 1710-1726.
62. Ariyasu J., Seaton C.T., Stegeman G.I., Appl.Phys.Lett., 1985, v. 47, p. 355-357.
63. Stegeman G.I., Seaton C.T., Ariyasu J., Wallis R.F., Maradudin A.A. J.Appl.Phys., 1985, v. 58, p. 2453-2459.
64. Jain R.K., Lind R.C. J.Opt.Soc. Am., 1983, v. 73, p. 647.
65. Chemla D.S., Miller D.A.B., Smith R.W. Opt.Eng., 1985, v. 24, p. 556.
66. Mathew J.G.H., Kar A.J., Heckenberg N.R., Galbraith I. I.E.E.E.J. Quantum Electron, 1985, v. 21, p. 774.
67. Yao S.S., Karaguleff C., Gabel A., Fortenberry R. et al. Appl.Phys.Lett., 1985, v. 46, p. 801-802.
68. Langbein V., Lederer F., Peschel T., Ponath H.E. Opt.Lett., 1985, v. 10, p. 571-573.
69. Stegeman G.I., Seaton C.T., Ariyasu J., Shen T.P., Moloney J.V. Opt.Comm., 1986, v. 56, p. 365.
70. Бойко Б.Б., Джилалдари Н.З., Петров Н.С. Ж.П.С. 1975, т. 23, с. 888-892.
71. Marcuse D. Appl.Opt., 1980, v. 19, p. 3130-3139.
72. Smith P.W., Tomlinson W.J. I.E.E.E.J. Quantum Electron, 1984, v. 20, p. 30-36.
73. Gardner C., Greene J., Kruskal M., Miura R. Phys.Rev. Lett., 1967, v. 19, p. 1095-1098.
74. Захаров В.Е., Шабат А.Б. ЖЭТФ, 1971, т. 61, с. 118-134.
75. Ames W.F. Nonlinear partial differential equations in engineering (Academic Press, N.Y., 1965).
76. Greenspan D. Discrete numerical methods in physics and engineering (Academic Press, N.Y., 1974).
77. Колоколов А.А. ЖИМ ТФ, 1973, т. 3, с. 152-155.
78. Mills D.L., Subbaswamy K.R. Progress in Optics, 1981, v. 19, ed. E.Wolf (North Holland, Amsterdam), p. 45.
79. Агранович В.М., Поверхностные поляритоны, под ред. Аграновича В.М. и Миллса Д.Л., М., Наука, 1985, с. 132-166.
80. Аланакян Ю.Р. ЖТФ, 1967, т. 37, с. 817-821.
81. Seaton C.T., Valera J.D., Svenson B., Stegeman G.I. Opt.Lett., 1985, v.10, p.149-150.
82. Agranovich V.M., Cernyak V.Ya. Phys.Lett., A, 1982, v. 88, p. 423-426.
83. Mihalache D. Solid St.Comm., 1986, v. 58, p. 125-127.
84. Ахмедиев Н.Н. ЖЭТФ, 1983, т. 84, с. 1907-1917.
85. Boardman A.D., Maradudin A.A., Stegeman G.I., Twardowski T., Wright E.M. Phys.Rev. A, 1987, v. 35, p. 1159-1164.
86. Берхофер А.Л., Захаров В.Е. ЖЭТФ, 1970, т. 58, с. 903-911.
87. Marcuse D. Theory of dielectric optical waveguides (Academic Press, N.Y., 1974).
88. Tien P.K. Rev.Mod.Phys., 1977, v. 49, p. 361-420.
89. Nolting H.P., Ulrich R. Integrated Optics. Springer Series in Optical Sciences, v. 48, 1985, Springer, Berlin.
90. Mihalache D., Mazilu D., Totia H. Phys.Scripts, 1984, v. 30, p. 335-340.
91. Mihalache D. Nonlinear Phenomena in Solids: Modern Topics, ed. M.Borissov, (World Scientific, Singapore, 1985), p. 99.
92. Mihalache D., Totia H. Solid St.Comm., 1985, v. 54, p. 175-177.
93. Seaton C.T., Valera J.D., Shoemaker R.L., Stegeman G.I. et al. I.E.E.E.J. Quantum Electron, 1985, v. 31, p. 774.
94. Boardman A., Egan P. I.E.E.E.J. Quantum Electron, 1985, v. 21, p. 1701.
95. Boardman A., Egan P. I.E.E.E.J. Quantum Electron, 1986, v. 22, p. 319-324.

96. Ахмедиев Н.Н., Болтарь К.О., Елеонский В.М. *Опт. Спектр.* 1982, т. 53, с. 906-909.
97. Ахмедиев Н.Н., Болтарь К.О., Елеонский В.М. *Опт. Спектр.*, 1982, т. 53, с. 1097-1103.
98. Михалаче Д., Федянин В.К. *ТМФ*, 1983, т. 54, с. 443-455.
99. Byrd P.F., Friedman M.D. *Handbook of elliptic integrals for engineers and physicists* (Springer, Berlin, 1954).
100. Stegeman G.I., Wright E.M., Seaton C.T., Moloney J.V. et al. *I.E.E.E.J. Quantum Electron*, 1986, v. 22, p. 977-983.
101. Fleck J.A., Morris J.R., Feit M.D. *Appl. Phys.*, 1976, v. 10, p. 129.
102. Fleck J.A., Morris J.R., Bliss E.S. *I.E.E.E.J., Quantum Electron*, 1978, v. 14, p. 353.
103. Ushioda S. *Progress in Optics*, v. 19, ed. E. Wolf (North-Holland, Amsterdam, 1981), p. 139.
104. Абелес Ф., Лопез-Риос Т. *Поверхностные поляритоны*, под ред. Аграновича В.М. и Миллса Д.Л., М., Наука, 1985, с. 167-189.
105. Stegeman G.I., Seaton C.T. *Opt. Lett.*, 1984, v. 9, p. 235-
106. Stegeman G.I., Valera J.D., Seaton C.T., Sipe J., Maradudin A.A. *Solid St. Commun.*, 1984, v. 52, p. 293-297.
107. Lederer F., Mihalache D. *Solid St. Commun.* 1986, v. 59, p. 151-153.
108. Mihalache D., Mazilu D., Lederer F. *Opt. Commun.*, 1986, v. 59, p. 391.

Received by Publishing Department
on January 25, 1988.

Михалаче Д., Назмитдинов Р.Г., Федянин В.К. E17-88-66
Нелинейные оптические волны в слоистых структурах

Рассматривается современное состояние проблемы распространения нелинейных оптических волн через диэлектрические и металлические слоистые структуры. Обсуждаются основные концепции и теоретические подходы, используемые при анализе нелинейных поверхностных волн (НПВ) и нелинейный волноводных мод (НВМ), амплитуды которых являются решениями определенного класса нелинейного уравнения Шредингера с коэффициентами, зависящими от поперечной координаты. Методами численного анализа проведено исследование устойчивости НПВ и НВМ. Предложены возможные приложения явления НПВ и НВМ для создания приборов нелинейной интегральной оптики.

Работа выполнена в Лаборатории теоретической физики ОИЯИ.

Препринт Объединенного института ядерных исследований. Дубна 1988

Mihalache D., Nazmitdinov R.G., Fedyanin V.K. E17-88-66
Nonlinear Optical Waves in Layered Structures

Modern status of the problem of propagation of nonlinear optical waves through dielectric and metallic layered structures is reviewed. The basic concepts and theoretical approaches used to analyse nonlinear surface and guided wave phenomena in planar structures are discussed. The amplitudes of these waves are obtained as special solutions of a nonlinear Schrodinger-like equation with coefficients that depend on the transverse coordinate. The stability of these new nonlinear optical waves to propagation in two- or three-layered planar structures is also numerically analysed. Some possible applications to integrated all-optical devices are suggested on the basis of these new nonlinear surface-guided waves.

The investigation has been performed at the Laboratory of Theoretical Physics, JINR.

Preprint of the Joint Institute for Nuclear Research. Dubna 1988